The Thesis Committee for Alex Edward Resovsky
Certifies that this is the approved version of the following thesis:

Effects of Simulated Inundation on Wetland Methane Flux Predictions for the Southeastern U.S.

APPROVED BY
SUPERVISING COMMITTEE:

Supervisor:

Zong-Liang Yang

Timothy M. Shanahan

Daniel O. Breecker

Effects of Simulated Inundation on Wetland Methane Flux Predictions for the Southeastern U.S.

by

Alex Edward Resovsky, B.S.

Thesis

Presented to the Faculty of the Graduate School of

The University of Texas at Austin

in Partial Fulfillment

of the Requirements

for the Degree of

Master of Science in Geological Sciences

The University of Texas at Austin

August 2015

Dedication

This work is dedicated to my family, especially my parents, Kathryn and Edward, for their unconditional love and support in this pursuit, as in all others. It is also dedicated to my many friends throughout the world, past and present, who make every endeavor worthwhile.

Acknowledgements

This work would not have been possible without the persistent guidance and instruction of Liang Yang. To him I owe my sincerest gratitude. A good deal of technical assistance was also provided by Dr. Muhammad J. Shaikh, and I thank him wholeheartedly for his contributions. I also wish to thank my group members, many of whom saw this work through from beginning to end and happily offered their advice and instruction along the way. You guys have taught me what it means to be a scientist, and I can not thank you enough for your immeasurable contributions to my personal growth and professional development during my time at the University of Texas.

Abstract

Effects of Simulated Inundation on Wetland Methane Flux Predictions for the Southeastern U.S.

Alex Edward Resovsky, M.S. Geo. Sci.

The University of Texas at Austin, 2015

Supervisor: Zong-Liang Yang

This work provides an overview of factors that influence methane emissions from natural wetlands in the southeastern U.S. at seasonal and interannual timescales. It then examines simulations using CLM4Me, a methane biogeochemistry model run within CESM, through comparison with recently compiled flux estimations from remote sensing data. In addition, we assess how seasonal methane flux simulations in CLM4Me are affected by the use of alternative estimates of inundated land fraction. Inundation predictions are provided by DYPTOP, a TOPMODEL implementation which can be used to simulate the dynamics of wetland spatial distribution. Results may aid in future model development and in understanding the role of subtropical and temperate North American wetlands under future climate projections.

Table of Contents

Chapter One: Introduction

Methane (CH_4) is an important greenhouse gas, and the predominant source of natural methane is its production in wetland soils. Wetlands and marshes in the southeastern U.S. (SE-US) comprise over 40 million acres of land, or more than one-third of total continental U.S. (CONUS) wetland acreage, and may thus represent a significant component of the global climate system. CH_4 contributions from these systems remain difficult to quantify, however. Existing field measurements are lacking in both spatial and temporal coverage, inhibiting efforts to produce regional estimates through upscaling. Top-down constraints on emissions have been generated using satellite remote sensing retrievals of column CH_4 (e.g., Frankenberg et al., 2005, 2008, Bergamaschi et al., 2007, 2013, Bloom et al., 2010, Wecht et al., 2014), but such approaches typically require preexisting emissions estimates to discern individual source contributions.

Land Surface Models (LSMs) have the potential to produce reliable results, but such predictions rely on accurate representations of sub-grid scale processes responsible for emissions. Since net fluxes are governed by complex interactions between local environmental and biogeochemical factors including water table position, soil temperature, soil substrate availability and vegetation type, realistic flux simulations depend not only upon how such processes are resolved but how skillfully the land surface state itself is predicted by a given model.

Here we conduct a first-order assessment of CLM4Me, the methane biogeochemistry component of the Community Land Model version 4.5 (CLM4.5, hereafter referred to as CLM). The aim is to examine the performance of CLM4Me in simulating fluxes from subtropical wetlands (latitudes ~25° - 35°). The southeastern continental U.S. (SE-US) is selected as a testbed for this work. We focus on this area for several reasons. First, a high proportion of subtropical North American wetlands are located in this region, including emergent, shrub and forested swamps in riverine and deltaic floodplains and >15 million acres of freshwater, estuarine and salt marshes along

the Gulf of Mexico coast (Dahl and Stedman, 2013). Despite this, SE-US wetland CH_4 fluxes have not been extensively studied and large uncertainties surround existing estimates for the region. Second, improved understanding of wetland fluxes in this region will allow for better constraints on fluxes from other sources. More specifically, CH_4 emissions from anthropogenic sources in the central and southern U.S. have received increased attention in recent years due in part to enhanced natural gas production (e.g. Allen et al., 2013, Miller et al., 2013, Brandt et al., 2014). Third, the U.S. Gulf of Mexico coastal region is highly susceptible to relative sea level rise (Hammer-Klose and Thieler, 2001, NABCI, 2010, Parris et al., 2012). Further knowledge of the carbon balance of wetlands in the Gulf Coast region is critical to predicting future climate impacts associated with increased inundation, a likely impact of rising global mean sea level (Wong et al., 2014). Finally, SE-US wetlands are disappearing at an alarming rate, primarily due to land-use and land-cover change. As an example, the Gulf Coast experienced net coastal wetland losses of 257,150 acres between 2004 and 2009. This accounted for 71% of all estimated wetland loss in U.S. coastal watersheds during this same period (Dahl and Stedman, 2013). This work will allow for better assessment of the effects of these changes on total global greenhouse gas (GHG) radiative forcing.

We begin by discussing the various process-level and ecosystem-level controls on CH_4 production in wetland soils. We then characterize the study domain for this work and describe the wetland habitat types prevalent throughout the southeastern U.S. Next, we review existing estimates for wetland CH_4 fluxes for the region based on top-down inversions and upscaled field measurements. Following this is a review of various modeling approaches for representing processes controlling wetland CH_4 fluxes at regional to continental scales.

In our subsequent discussion of how various ecological processes and CH_4 transport mechanisms are explicitly resolved in CLM4Me, we stress the relative importance of water table depth as a process- and ecosystem-level control. This provides

context for the experimental results, where examine the effects of changes in SE-US inundated land fraction as calculated by the Dynamical Peatland Model Based on TOPMODEL (DYPTOP). Analysis of the experimental results allows us to assess possible implications for future CH_4 flux module design in LSMs.

1.1 Overview of wetland methane production

CH_4 in soils is produced as methanogenic bacteria decompose soil organic matter. Because these bacteria require anoxic conditions in order to grow, saturated soils such as those found in wetland environments provide ideal conditions for methanogenesis (as the presence of water inhibits the diffusion of oxygen into the soil). However, much of the CH_4 produced is subsequently oxidized in surficial oxic soil layers during transport to the surface (Whalen, 2005). Net emissions therefore reflect the balance between CH_4 production and consumption in the soil column, processes which are carried out by different functional groups of bacteria (EPA, 2010).

Once the prerequisite of anoxic conditions is met, the efficiency of methanogenesis and the resulting surficial CH_4 flux are further determined by a range of environmental variables, which are classified here into two types of controls: process-level and ecosystem-level controls (after Whalen, 2005). Process-level controls are those which affect how well bacteria thrive in the soil column, and include the quality and quantity of soil organic material, soil pH and temperature. Ecosystem-level controls are related to the relative efficiency of different CH_4 transport pathways and include water table position, vegetation type and climatic setting. Figure (1) shows various controls on CH_4 formation at different spatial and temporal scales.

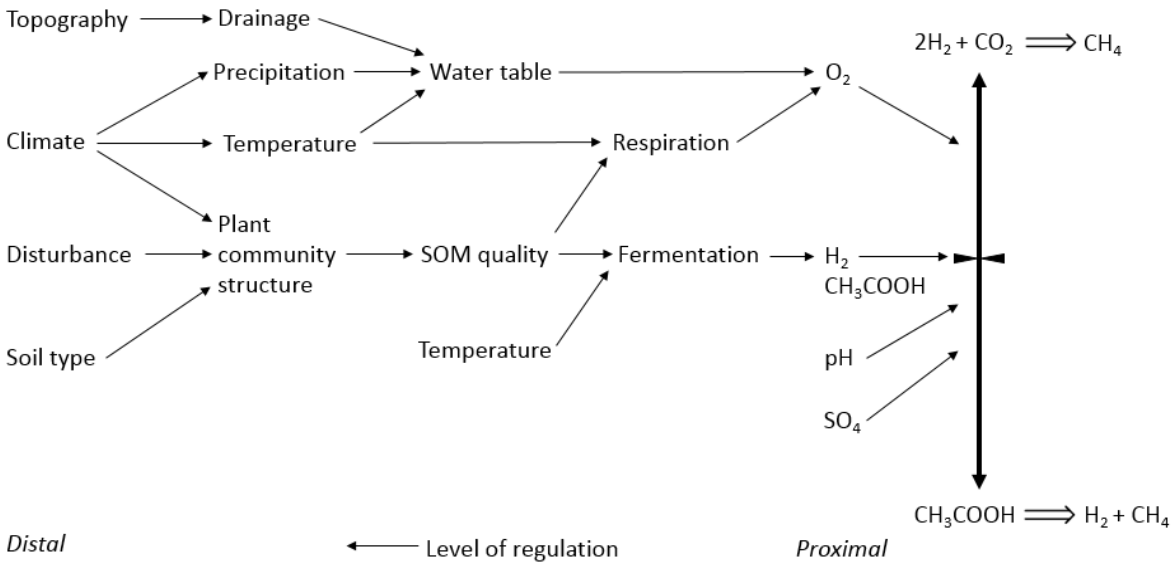

Figure 1: Major controls on the pathways to CH_4 formation (adapted from Christensen, 2010).

1.1.1 Process-level controls

Process-level controls are variables that influence the biogeochemical reactions related to CH_4 production and oxidation. However, since bacterial responses to fluctuations in these factors are often complex and non-linear, fluxes can vary greatly both spatially and temporally. Accurate spatial data for such parameters as soil temperature and pH are also sparse, complicating attempts to understand the role of such factors at regional scales.

Substrate type and availability. Since CH_4 is produced through the decomposition of soil organic material (substrate), the quality and availability of organic compounds act as first-order controls on methanogenesis (e.g., Bridgham and Richardson, 1992, Boon and Mitchell, 1995). Acetate in particular is an important precursor for CH_4 formation and its amendment has been shown to strongly enhance methanogenesis in peats (Goodwin and Zeikus, 1987, Christensen et al., 2003). Other soil compounds may inhibit CH_4 production. For example, the addition of sulfur may

alter carbon flow pathways and reduce the energy flow through methanogenesis, since SO_4 may also be used by bacteria to decompose organic material (Schimel, 2004, EPA, 2010).

pH. Empirical studies have shown that maximum rates of CH_4 production tend to occur at or near neutral pH conditions (e.g. Dunfield et al., 1993; Zhuang et al., 2004). However, some evidence suggests that CH_4 may also be produced under acidic conditions; Svensson and Roswell (1984) and Goodwin et al. (1988) showed that sediments incubated at acidic pH continued to produce CH_4, and methanogenesis has been observed at pH as low as 4.0 in northern bogs (Williams and Crawford, 1985; Valentine et al., 1994) and 3.1 from an isolated strain of methanogenic bacteria in a laboratory experiment (Williams and Crawford, 1985).

Valentine et al. (1994) and Bergman et al. (1998) observed differences in the sign of methanogenic response to increased pH in different peat types. They attributed these differences to pH-induced changes in microbial community structures. Despite the range of results, Moore and Roulet (1995) suggest that pH is a secondary factor in determining wetland CH_4 emission, as strongly acidic peats may show high or low CH_4 fluxes.

Temperature. Some reported Q_{10} temperature coefficients for methanogenesis (where Q_{10} signifies the reaction rate increase for a 10°C temperature increase) have indicated a strong methanogenic response to temperature change relative to other biochemical reactions (EPA, 2010). Christensen et al. (2003) confirm that mean seasonal soil temperature acts as a strong predictor for CH_4 flux rates and, with an exponential correlation, explains up to 84% of the variance in CH_4 emissions.

Reported Q_{10} values for methanogenesis vary greatly between studies, however. This variance may in part be attributed to such factors as experimental temperature range (Yavitt et al., 1997), depth of sample collection (McKenzie et al., 1998), and season (Yavitt et al., 2000). Furthermore, it is unlikely that empirical observations are indicative

of the true physiological temperature response of methanogenesis. Rather, the wide range of reported values likely reflects the temperature sensitivity of the underlying microbial processes involved in the production of methanogenic precursors under subsaturated substrate conditions, since these processes limit the temperature response of methanogens (Whalen, 2005). For instance, temperature response experiments involving the addition of methanogenic substrates (Westermann, 1993) or precursors (Bergman et al., 1998) under carefully controlled conditions show that reported Q_{10} values for methanogenesis in natural soil samples are highly sensitive to instantaneous substrate conditions. In addition, cultured methanogens (without substrate limitation) show a surprisingly wide range of Q_{10} values (Segers, 1998), suggesting high intrinsic variability among species with respect to the temperature influence on growth.

In general, methanogens are mesophilic, having a temperature optimum for growth in the 30° to 40°C range. The optimum temperature range for methanogenesis has been found to be anywhere from 20° to 25°C in subarctic peats (Svensson, 1984, Dunfield et al., 1993) to between 35° and 40°C in temperate lake sediments (Zeikus and Winfrey, 1976).

1.1.2 Ecosystem-level controls

In general, wetland soils are stratified vertically into two layers: a saturated zone and an overlying subsaturated zone (Figure 2). CH_4 is produced in the anoxic, water-saturated zone and may be transported upward through one of several processes. Primary transport pathways include (1) diffusion, where CH_4 produced in the water-saturated zone is transported to the air–water interface by aqueous phase molecular diffusion, (2) ebullition, which describes the episodic release of bubbles of trapped free-phase gas from the soil directly to the atmosphere resulting from changes in atmospheric temperature, pressure, and/or water table elevation, and (3) plant-mediated transport, whereby gas transfuses to the surface via connected pore spaces within the roots and stems of wetland plants.

Ecosystem-level controls affect the importance of each of these transport mechanisms, and play a role in determining how much of the total CH_4 produced in the soil column is subsequently released to the atmosphere.

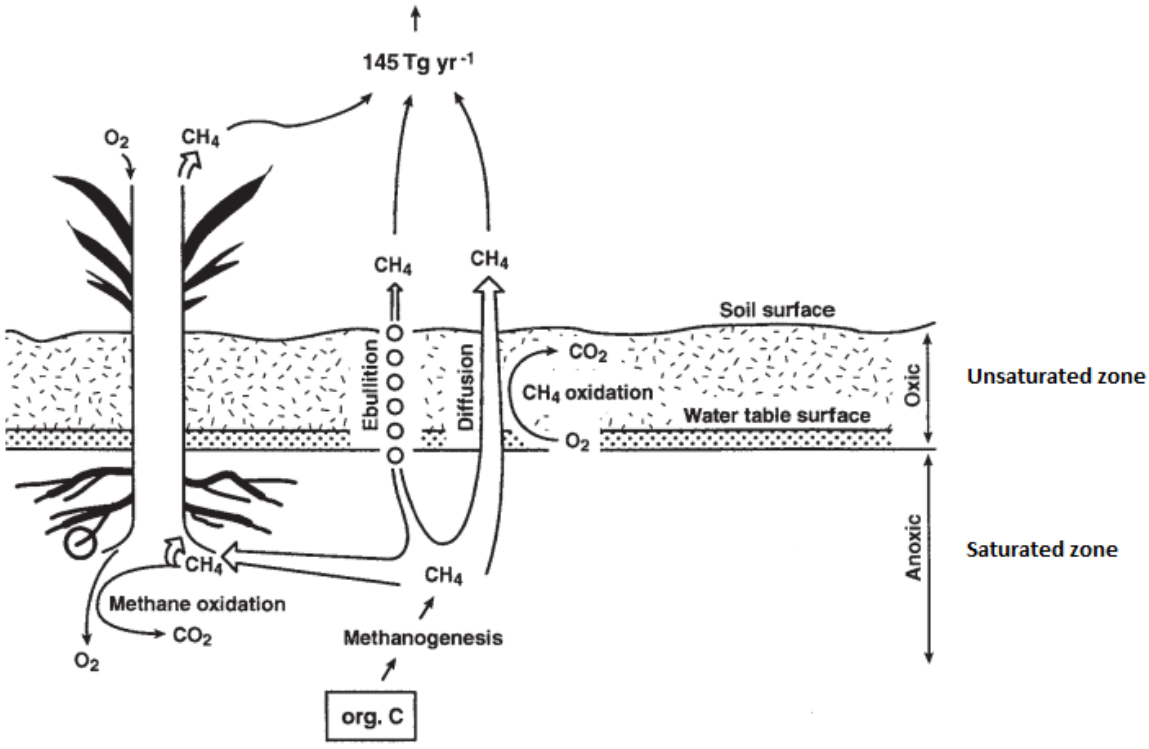

Figure 2: Conceptual model of CH_4 cycling in wetland environments, showing plant-mediated transport, ebullition, and diffusion (adapted from Whalen, 2005).

Water table position. In conceptual wetland CH_4 models, CH_4 produced in the anoxic, saturated soil zone becomes oxidized (consumed) by methanotrophic bacteria in the subsaturated soil layer as it diffuses upward. Observed CH_4 profiles in peats support this concept, with CH_4 concentrations consistently three to five orders of magnitude higher in the saturated zone than in the overlying unsaturated zone. When the water table is at the soil surface, CH_4 oxidation is restricted to a small oxygenated zone. A reduction

of the water table increases the vertical extent of the zone of CH_4 oxidation, while decreasing the zone of methanogenesis (Whalen, 2005).

These effects imply that seasonal fluctuations in water table position can strongly influence net CH_4 emission and uptake in wetland soils. Indeed, several studies have found increases in CH_4 consumption in wetlands as a result of water table drawdown (e.g., Glenn et al., 1993, Roulet et al., 1993, Laine et al., 1996). Likewise, Hariss et al. (1982) found that a seasonal reduction in water table position transformed a temperate swamp from an atmospheric CH_4 source to a sink.

Vegetation communities. Plants have been shown to affect CH_4 emissions both directly and indirectly. Firstly, some wetland plant species can transport gases produced in sediments such as CH_4 directly to the air through soft tissue known as aerenchyma (Sebacher et al., 1985). This same mechanism may be responsible for the downward transport of oxygen into the soil column, which may impact CH_4 oxidation. In addition, species differ in the amount of biomass they produce, as well as how easily that biomass may be decomposed (EPA, 2010).

Vascular plants which transmit CH_4 through their stems and leaves allow CH_4 produced in the saturated soil zone to bypass the near-surface zone of CH_4 oxidation. In some wetland types, this pathway is responsible for a significant portion of the total flux; Schimel (1994) found that plant-mediated transport was the dominant transport pathway for CH_4 produced in arctic sedges, while Whiting and Chanton (1992) studied CH_4 emissions from sub-arctic fens and estimated that 90% were plant-mediated.

Total plant biomass production and decomposition rates have also been linked to CH_4 emission. For example, Whiting and Chanton (1993) found a strong correlation between total carbon fixation and net fluxes in wetland ecosystems. However, since other soil factors such as the presence of sulfate reducers and the nitrogen content of the soil can affect the relative carbon flow through methanogenesis, efforts to estimate CH_4

emissions based on net ecosystem production (e.g. Potter et al., 2006) may benefit from improved representations of such fine-scale biophysical controls.

Climatic setting. Regional climatic setting can influence hydrologic conditions and other state variables, including plant primary productivity and soil temperature. In the tropics for example, rates of primary production are typically high since temperatures and insolation are higher throughout the year. Rates of decomposition in tropical wetlands may also be quite high (Bartlett and Harriss, 1993), resulting in greater nutrient availability. Tropical wetland areas may also be subject to significant seasonal changes in the extent of inundation, as the amount of precipitation varies throughout the year.

Subtropical and temperate wetlands in North America likewise experience seasonality in inundation extent, as well as strong seasonal shifts in soil temperature, which have been linked to annual flux patterns (Crill, 1991). At higher latitudes, CH_4 produced in winter can become trapped in frozen soil and released during the spring thaw period, which may result large seasonal pulses in emissions (Hargreaves et al. 2001).

Climate conditions can also impact the physical transport of CH_4. For instance, Tokida (2007) found that local decreases in atmospheric pressure can cause sudden pulses in emissions. This occurs as the reduced air pressure allows bubbles containing free-phase CH_4 gas to escape to the surface without being oxidized (ebullition). Soil moisture content, which is influenced by local meteorologic and climatic processes, may also have a strong impact on CH_4 diffusion rates, since it influences the interconnectivity of air-filled pore space in the soil.

1.2 Wetland habitats of the southeastern U.S.

1.2.1 Overview, characteristics and spatial distribution

The SE-US (here defined as encompassing east Texas and the states of Arkansas, Louisiana, Tennessee, Mississippi, Alabama, Virginia, North and South Carolina,

Georgia and Florida) represents a significant fraction of U.S. wetlands, with the five Gulf Coast states alone containing more than 32% of total CONUS wetland acreage (Dahl, 2005, 2011, USDA, 2013). Much of this acreage occurs within the low-lying Atlantic Gulf Coastal Plain, including >15 million acres of wetlands in Gulf Coast watersheds. These coastal wetlands include primarily freshwater, estuarine and salt marshes, along with bottomland hardwood swamps, mangrove swamps, and shrubby depressions known in the southeastern U.S. as "pocosins" (NOAA). Notable coastal wetland habitats include the greater Everglades in southern Florida, an expanse of marsh and swampland extending throughout southern and southwestern Florida encompassing nearly 750 square miles. A particularly large assemblage of coastal wetlands exists in southern Louisiana, where more than 4,000 square miles of freshwater, intermediate and saline marshes are found, many within the deltaic floodplain of the Mississippi River (USFWS, 2014).

In addition, the lower Mississippi Valley features more than 7,000 square miles of freshwater forested and shrub wetlands in watersheds adjacent to the Mississippi River floodplain (USFWS, 2014). These areas occur throughout north-central Louisiana, northwest Mississippi and eastern Arkansas and their presence is strongly influenced by fluctuations in river and stream flow as a result of varying precipitation. Floodwaters in this region may inundate floodplains and fill pools and backwaters before subsiding and leaving much of the floodplain relatively dry for varying periods between floods (Godfrey and Wooten, 1981). Other major wetlands in the southeastern coastal plain include the Okefenokee Swamp in Georgia and Florida and the Great Dismal Swamp in Virginia and North Carolina. The former covers more than 600 square miles and consists of peat-floored blackwater marshes containing hardwood and shrub communities interspersed with lakes and wet prairies. The Great Dismal Swamp encompasses 170 square miles of upland woods, open water and marshland along the North Carolina-Virginia border (Shaw, n.d.).

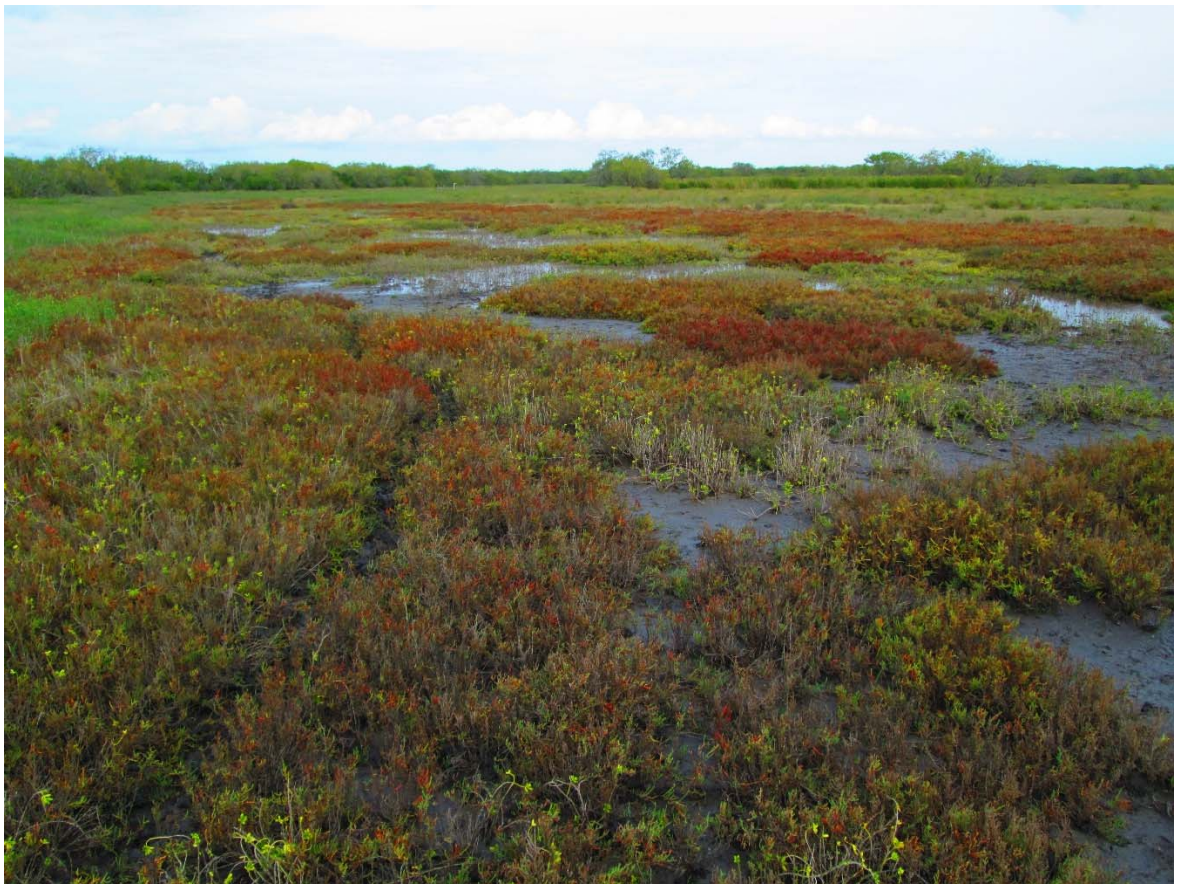

Figure 3: A coastal marshland near Corpus Christi, Texas (photo by author).

Wetland regions such as these have experienced extensive habitat loss due to conversion of land for agriculture and for residential and other development. The Great Dismal Swamp, for example, once covered more than 1,500 square miles. Recent surveys conducted by the U.S. Fish and Wildlife Service (e.g., Dahl and Stedman, 2013) show wetland habitat losses continue today, though this trend may change as more wetlands in the southeast are conserved as protected natural areas. At present however, current rates of wetland loss subject interannual CH_4 emissions estimates from the region to additional uncertainty.

1.2.2 Existing SE-US wetland methane estimates: Bases for comparison with this study

Verification of model predictions by comparison with observational data, where available, is integral to the development of any LSM component. Although direct wetland CH_4 flux observations at the land surface have historically been limited in spatial and temporal extent, a meta-analysis of existing site-scale studies in the literature may provide a basis for large-scale emissions estimates. For example, Bartlett and Harriss (1993) reviewed several small-scale measurement studies in the continental U.S., mostly conducted at wetland sites in the southeast. From these studies, they calculated an average emission figure for temperate forested swamps of 75 mg CH_4/m^2/day and for temperate non-forested swamps of 70 mg CH_4/m^2/day. Using their estimated emission season, which corresponds roughly to the annual period of warm temperatures (assumed to be 150 days per year for wetlands between 30° and 45°N and 180 days for those south of 30°N), annual CH_4 fluxes for the SE-US can be estimated using, e.g., acreages surveyed in the National Wetlands Inventory (NWI, USFWS, 2014). This method gives an annual flux of approximately 2.2 Tg CH_4 from SE-US wetlands given the total SE-US acreages of three NWI wetland classifications: estuarine and marine wetlands, freshwater forested/shrub wetlands, and freshwater emergent wetlands.

It is important to note that average flux rates are not entirely representative of the high annual and interannual variability associated with wetland CH_4 emissions. Measured CH_4 fluxes can vary greatly between locations within the same study area as a result of microtopographic influences on surface water and changes in biogeochemistry (Bubier et al., 1993, Bubier et al., 1995). Indeed, most of the studies analyzed by Bartlett and Harriss (1993) report a range of annual emissions for subtropical- and temperate-latitude wetlands over one to two orders of magnitude (in g/m^2/yr). For this reason, other attempts to estimate regional emissions for the SE-US have focused on correlations between observable large-scale ecosystem-level parameters and net emissions. For

example, Potter et al. (2006) assimilated satellite-derived vegetation "greenness" index values into a wetland ecosystem model to generate nationwide estimates of net ecosystem production (NEP) for the U.S. They then multiplied these values by a CH_4 : CO_2 conversion factor determined by Whiting and Chanton (1993) to derive wetland fluxes for the continental U.S. Their results indicate that the southeast contributes 3.0 Tg of wetland CH_4 annually. We note that this figure includes the entire state of Texas, and since only east Texas is considered part of the study area for this work, this total for SE-US wetlands based on Potter et al. (2006) may be slightly lower.

Other, more recent estimates have been based on analyses of direct atmospheric concentration measurements. For illustration, optimized North American CH_4 emissions derived from atmospheric column satellite retrievals by Wecht et al. (2014) are shown below. Results from Wecht et al. (2014) indicate similar ranges of fluxes as given by the above-mentioned methodologies, and show a predictable spatial pattern for North American wetland emissions that includes an expected anomalous region of high flux over the southeast (Figure 4). To deduce CH_4 sources, "top-down" or inversion approaches (e.g., Frankenberg et al., 2005, Bergamaschi et al., 2007, Bloom et al., 2010) such as these rely on a combination of *a priori* emissions inventories, atmospheric transport models and data on atmospheric hydroxl radical (OH^-) concentrations (since OH^- molecules oxidize CH_4 and thereby remove it from the atmosphere). Such work may serve as a useful reference for comparison with LSM results, and we examine these estimates in further detail in section 2.3.

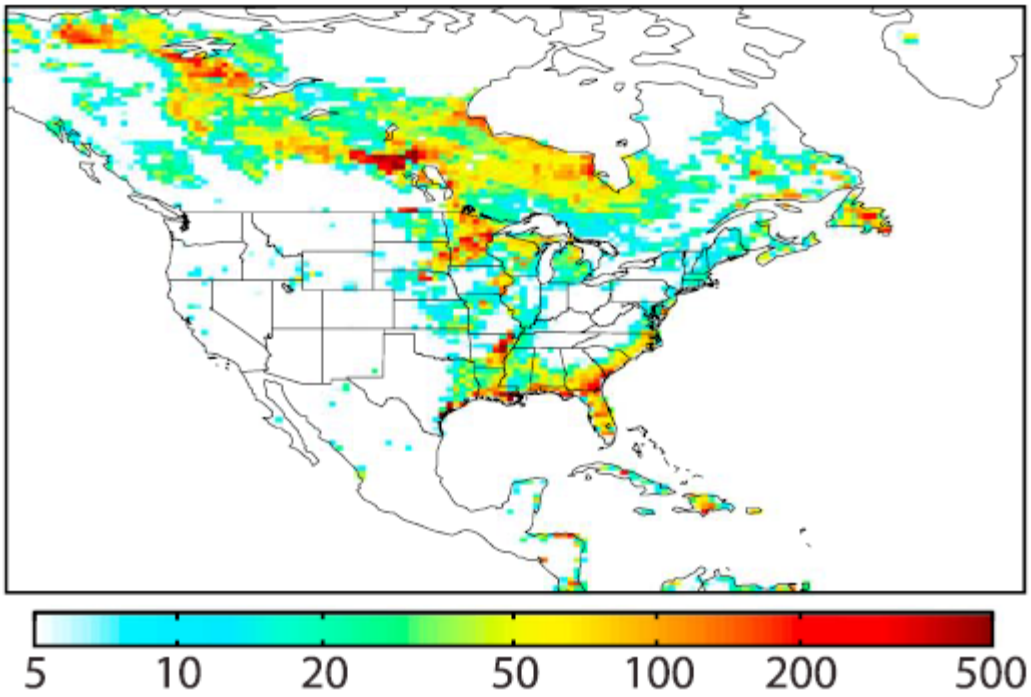

Figure 4: North American wetland CH_4 emissions for the year 2004 (10^{10} molecules/cm^2/s) from Wecht et al. (2014) at 1/2° lat x 2/3° lon resolution using SCIAMACHY retrievals of atmospheric column CH_4. Emissions are optimized via a clustering algorithm based on the emissions inventories of Kaplan et al. (2002) and Pickett-Heaps et al. (2011). Conversion factor: 10^{10} molecules/cm^2/s = 6.284×10^{-14} Tg C/m^2/yr.

1.3. Model representation of wetland ecosystem processes

Mechanistically modeling net surface CH_4 emissions requires representing a complex and interacting series of ecological and biogeochemical processes. A diverse suite of ecosystem CH_4 modeling approaches has been developed for application to wetland soils. These include (1) empirical models, or simulations based on regression analyses of CH_4 fluxes on soil temperature, soil moisture content, water table depth, pH measurements and other physical parameters, and (2) process-based models. In empirical CH_4 flux models, regressions are used in combination with soil climate models in order to predict daily CH_4 fluxes at or near sites where soil parameters have been measured directly at the surface. Flux simulations based on these regressions, however, may not be

applicable to locations outside of the measurement area, where conditions differ. Process-based models, meanwhile, use an understanding of biogeochemical and environmental controls and their interactions to calculate CH_4 fluxes. They have the advantage of being more broadly applicable since they are not statistically based, though they often require rigorous testing and calibration. We focus here on the latter type, which includes CLM4Me.

In general, process-based CH_4 biogeochemical modeling approaches can be characterized hierarchically according to their complexity (e.g. Grant and Roulet, 2002). They include: (1) mechanistic representations where daily CH_4 fluxes are simulated from calculated rates of organic matter and litterfall decomposition, modified by soil conditions such as redox potential, pH, temperature, nutrient status, and water table depth (e.g., Cao et al., 1995, Potter et al., 2001); (2) models applied at site, regional, and global scales that explicitly represent processes for microbiological transformations and physical transport of CH_4 (Figures 5 and 6) including aqueous and gaseous transport and competition between processes affecting CH_4 concentrations (e.g., Walter et al., 2001, Zhang et al., 2002; Zhuang et al., 2004); (3) simulations that explicitly resolve the three CH_4 transport mechanisms, include representations of the production and consumption of CH_4 in the soil column by different microbial groups and account for how these microbes interact with substrates, pH, and redox potential (e.g., Grant, 1998, 1999).

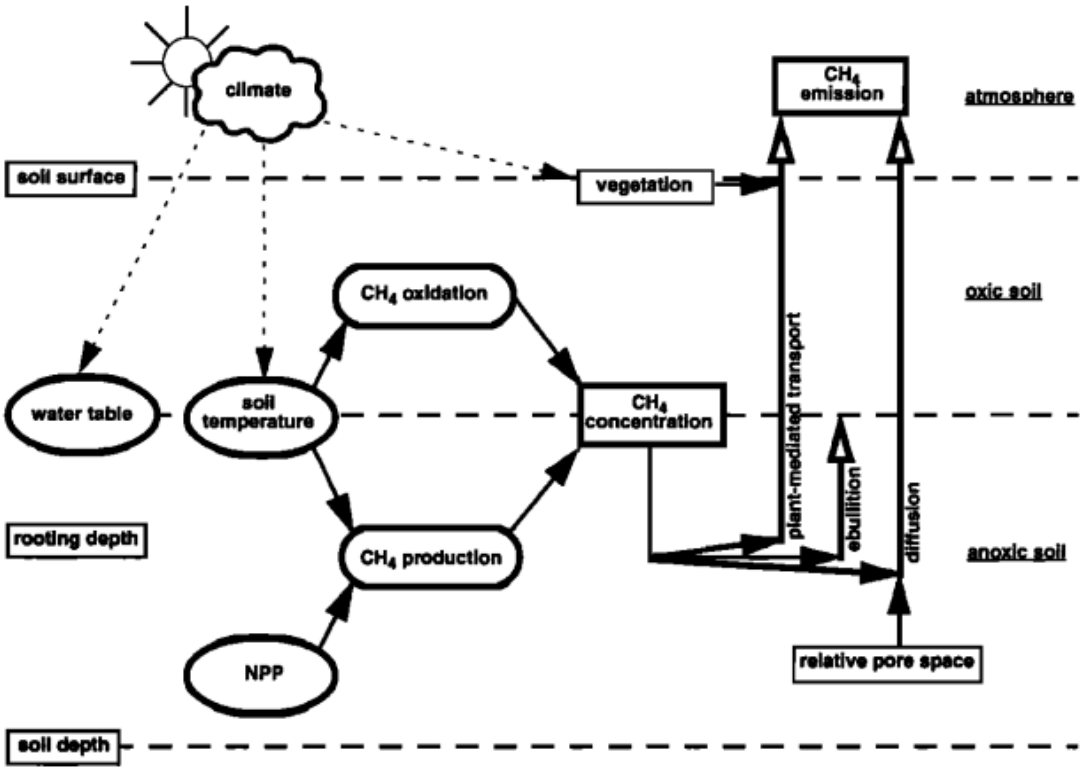

Figure 5: (Top) Schematic of the one-dimensional CH_4 model of Walter et al. (2001); CH_4 production takes place in the anoxic soil below the water table; the CH_4 production rate depends on soil temper-ature and NPP. CH_4 oxidation occurs in the oxic soil above the water table and depends on temperature. The model calculates CH_4 concentrations in each (1 cm thick) soil layer. Transport occurs by diffusion through water-/air-filled soil pores, ebullition to the water table, and plant-mediated transport from layers above the rooting depth.

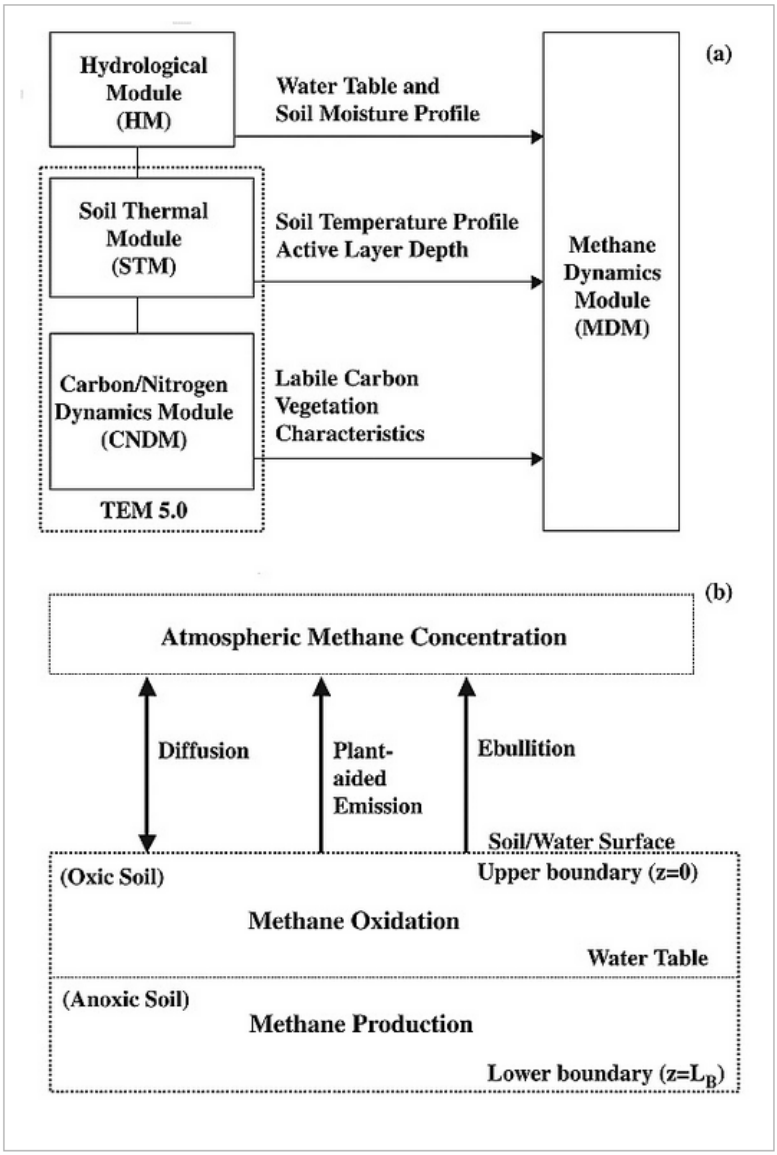

Figure 6: Schematic diagram of Zhuang et al.'s biogeochemistry model (TEM), showing (a) the overall model structure which features a soil thermal module, a hydrologic module, a carbon/nitrogen dynamics module, and a CH_4 dynamics module (MDM), and (b) the more detailed structure of the MDM including the separation of soil into anaerobic and aerobic zones by water table position. The soil profile is divided into 1-cm layers. Parameterizations of the different transport pathways of CH_4 between soils and the atmosphere (diffusion, plant-aided transport, and ebullition) are described in greater detail in Zhuang et al. (2004).

The results of process-based model experiments (e.g. Cao et al., 1996) suggest that such models have the potential to capture overall seasonal trends in emissions quite well, at least for some wetland sites. However, magnitudes of year-to-year fluxes have proven difficult to predict accurately. Furthermore, sensitivity analyses indicate that predictions are highly sensitive to specified values for parameters such as water table position and temperature. Zhang et al. (2002), for example, show that different parameterizations of the effects of temperature, hydrologic dynamics, and soil organic C content can strongly influence flux predictions in process-based models. Melton et al. (2013), meanwhile, conducted an inter-comparison study of several process-based wetland CH_4 models and found broad disagreement between them. Differences were found to be reflective of the models' respective schemes employed for calculation of inundated land surface fraction, taken to indicate wetland areal extent.

Such findings imply that assimilation of observational data may allow for improvement in predictive skill (e.g. through tuning of model parameters). In the past, however, wetland CH_4 observational datasets have tended to be largely insufficient for evaluation of model fluxes at regional spatial scales, and datasets often do not contain contemporary and co-spatial measurements of soil and hydrological states that might facilitate tuning. In the following section, we examine a particular process-based CH_4 biogeochemistry model, CLM4Me (Riley et al., 2011), and describe the model-specific parameterizations used in calculation of net surface CH_4 flux from wetland soils. We focus especially on the current methodology for calculation of wetland areal extent in CLM4Me and briefly discuss CLM4Me-generated inundation patterns over the study area. We then evaluate the overall performance of CLM4Me over the study region by comparing simulations to newly-available flux estimates from satellite remote sensing measurements.

Chapter Two: Datasets and Methodology

2.1 Wetland methane flux prediction in CLM4Me

Although accurate representations of every sub-gridscale process important to CH_4 production and transport is preferable in the development of a mechanistic model, several limitations must be considered. These include (1) uncertainties in assumed system structure, (2) uncertain parameter characterization, (3) uncertainties associated with spatial heterogeneity, (4) limited availability of measurements to develop, test, and perform simulations (as discussed in section 1.3), (5) uncertainties in boundary and initial conditions, and (6) a need for computational efficiency. All of these restrictions are relevant to CLM4Me.

In the model structure, constraints on several important model parameters are provided by the current literature, such as soil half-saturation coefficients and maximum potential rate for oxidation, temperature dependence of methanogen productivity, the effects of competition between processes (e.g. aerenchyma transport vs. oxidation by methanotrophs in the soil), and the spatial distributions of state variables affecting CH_4 production and oxidation (e.g., pH, redox potential, inundation) (Riley et al., 2011).

CLM4Me simulates the transient, vertically resolved dynamics of CH_4 and oxygen in the soil column (Figure 7). For CH_4, the model accounts for production in the anaerobic fraction of soil (P, mol/m^3/s), ebullition (E, mol/m^3/s), aerenchyma transport (A, mol/m^3/s), aqueous and gaseous diffusion (F_D, mol/m^2/s), and oxidation (O, mol/m^3/s) via a transient reaction diffusion equation:

$$\frac{\partial(RC)}{\partial t} = \frac{\partial F_D}{\partial z} + P(z,t) - E(z,t) - A(z,t) - O(z,t) \quad (1)$$

Where z (m) represents the vertical dimension, t (s) is time, and R accounts for gas in both the aqueous and gaseous phases: $R = \varepsilon_a + K_H\varepsilon_w$, with ε_a, ε_w, and K_H (−) the air-filled porosity, water-filled porosity, and partitioning coefficient for the gas species of interest, respectively. An analogous version of Equation (1) is concurrently solved for oxygen, but with the following differences relative to CH_4: $P = E = 0$ (i.e., no production or ebullition), the aerenchyma transport is a source rather than a sink, and the oxidation sink includes the oxygen demanded by methanotrophs, heterotrophs, and autotrophic root respiration (Riley et al., 2011).

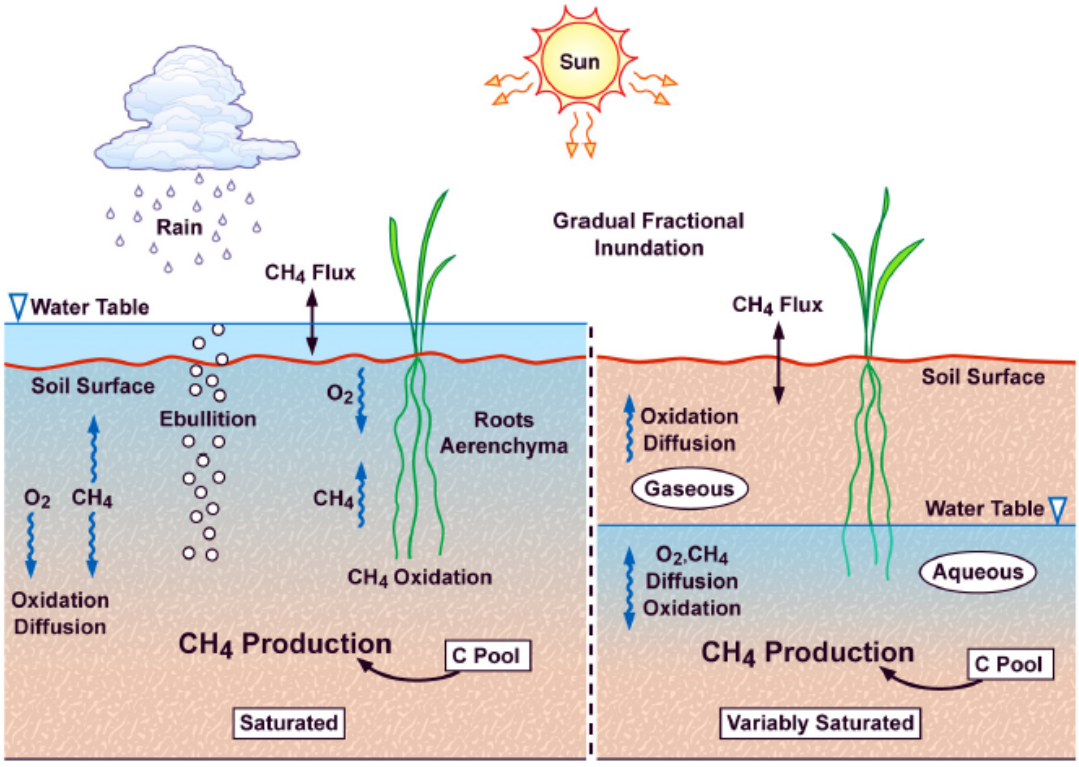

Figure 7: Schematic representation of biological and physical processes integrated in CLM4Me that affect the net CH_4 surface flux. (Left) Fully inundated portion of a CLM gridcell and (right) variably saturated portion of a gridcell (Riley et al., 2011).

Since CLM does not have a specific wetland representation that includes details relevant to CH_4 production, gridcell-averaged decomposition rates are used as proxies for wetland CH_4 fluxes. CH_4 production in the anaerobic portion of the soil column is related to the gridcell estimate of heterotrophic respiration from soil and litter (R_H; mol $C/m^2/s$) corrected for its soil temperature (T_s) dependence, soil temperature through a Q_{10} factor (f_T), pH (f_{pH}; Meng et al., 2011), redox potential (f_{pE}), and a factor accounting for the seasonal inundation fraction (S):

$$P = R_H f_{CH4} f_T f_{pH} f_{pE} S \quad (2)$$

where f_{CH4} is the baseline fraction of anaerobically mineralized C atoms becoming CH_4. The seasonal inundation fraction, S, is defined as

$$S = \frac{\beta(f-\overline{f})+\overline{f}}{f},\ S \leq 1. \quad (3)$$

where f is the instantaneous inundated fraction, $\overline{f}$ is the annual average inundated fraction weighted by heterotrophic respiration (evaluated for the previous calendar year), and β is an anoxia factor that relates the fully anoxic decomposition rate to the fully oxygen-unlimited decomposition rate, all other conditions being equal (Riley et al., 2011).

2.2 Determination of inundated fraction and wetland areal extent in CLM4Me

Since saturated soil conditions are required for methanogenesis, the spatial extent of inundation (the land surface area where water is present at the surface) acts as an important control on regional CH_4 emissions. Because static wetland datasets (e.g., Lehner and Döll, 2004, MODIS: ORNL DAAC, 2000, USFWS, 2014) do not adequately capture seasonal and interannual variations in inundation extent, their applications for CH_4 flux predictions in LSMs are somewhat limited.

To remedy this restriction, CLM4Me employs an approach intended to portray temporal variations in inundation extent. CLM4Me's inundation dataset is based on work by Prigent et al. (2007), who estimated global monthly inundated fraction from 1993–2000 using a multi-satellite approach. We refer to it here as the Global Inundation Extent from Multi-Satellite (GIEMS) dataset (after Melton et al., 2013). The GIEMS values are based on observed radiometric anomalies and Normalized Difference Vegetation Index (NDVI) values from the Advanced Very High Resolution Radiometer (AVHRR) in combination with passive microwave Special Sensor Microwave/Imager (SSM/I) measurements and active microwave backscattering coefficients at 5.25 GHz from the European Remote Sensing (ERS) satellite. This approach is described in greater detail in Prigent et al. (2001, 2007).

Initally, index values for the saturated fraction (f_s) of each gridcell are generated independently by CLM. These index values are computed from the model-simulated water table depth (z_w) and a spatially variable parameter representing surface runoff (Niu et al., 2005, Oleson et al., 2008). A simple inversion is then applied to these f_s values in CLM4Me, optimizing three parameters (p_1, p_2, p_3) for each gridcell to approximate the GIEMS values of Prigent et al. (2007). The optimization utilizes model-generated water table depth and surface runoff (Q_r (mm/s)):

$$f_i = p_1 e^{-z_w/p_2} + p_3 Q_r \quad (4)$$

Here, f_i represents the inundated fraction used specifically by the CH_4 submodel, calculated at each time step. Although the f_i values are designed to better reflect the spatiotemporal variability of the GIEMS dataset at the global scale, discrepancies still arise at local (gridcell to regional) levels (Riley et al, 2011). These errors are potentially important for CH_4 emissions estimates; for example, discrepancies occur in several important high-latitude wetland regions including northern Eurasia and mid- and eastern

Canada. Over the study region for this work (the SE-US), Riley et al. (2011) show a slight positive bias in f_i when compared to the multi-satellite values, particularly over the Mississippi River basin (Figure 8).

The GIEMS estimates themselves are complicated by several factors as well. For example, Prigent et al. (2007) note that the data do not discriminate among inundated wetlands, rivers, small lakes, irrigated agriculture or ocean-contaminated coastal pixels. Additionally, bare surfaces and inundation can produce similar SSM/I signatures in semiarid regions, complicating efforts to discern inundated areas (Prigent et al., 2007). Passive microwave signals may also be contaminated by atmosphere, clouds and rain, and signals can be altered by absorption and scattering by vegetation and modulated by surface temperature.

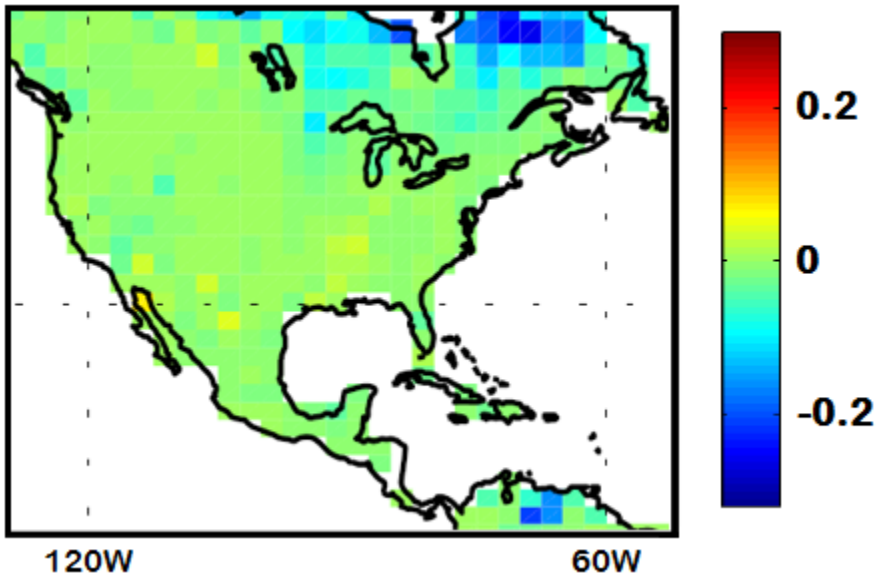

Figure 8: Difference between mean June–September observed inundation (GIEMS; Prigent et al., 2007) and inundation simulated by CLM (adapted from Riley *et al*., 2011).

2.3 DYPTOP dynamic inundation prediction

The TOPMODEL approach (Beven and Kirkby, 1979) accounts for several factors to predict runoff generation and areal extent of potential flooding in hydrological catchments. In TOPMODEL, areal units are assigned "floodability" index values according to their topography. Sub-grid scale topography information is used to resolve the redistribution of soil water within a river catchment so that the area at maximum soil water content can be determined. The area at maximum soil water content can then be used to implicitly represent the inundated area fraction.

The Dynamical Peatland Model based on TOPMODEL (DYPTOP, Stocker et al., 2014) applies this approach to establish a gridcell-specific relationship between the model-simulated water table depth (Γ) and the gridcell flooded area fraction (f). Once established, this grid-cell-specific relationship is represented by a single analytical function established using a set of four parameters (v, k, q, f^{max}). A global dataset of these four parameters at 1° x 1° gridcell resolution is provided by Benjamin Stocker at https://github.com/stineb/dyptop. The analytical function is used to dynamically predict f in combination with Γ as simulated by a land surface model. Stocker et al. (2014) note that this approach reduces required input data, enhances computational efficiency and allows for integration of the dynamical inundation prediction scheme into any LSM.

The global set of gridcell-specific functions developed using the four "fit" parameters v, k, q, and f^{max} is designed to approximate the "empirical" relationship between Γ and f for each gridcell. This empirical relationship is initially derived using a gridcell's respective sub-grid level Compound Topographic Index (CTI) values. CTI values are ascribed to each "pixel" within a gridcell (index i; for the 1° x 1° gridcells used in Stocker *et al*., pixels are ~1 km x 1 km) and reflect a pixel's floodability. The CTI values are derived from the ETOPO1 high resolution (1 arc min) topography dataset (Amante and Eakins, 2009) and are calculated using the R library "topmodel" (Buytaert, 2011).

A threshold value CTI^*_x is calculated for each gridcell *x* as a function of the grid-cell-mean water table position (Γ_x). All pixels with $CTI_i > CTI^*_x$ are assumed to be at maximum soil water content. The flooded area fraction of a gridcell *x* is then calculated as

$$f_x = \frac{1}{A_x}\sum_i A_i^* \tag{5}$$

$$\text{with } A_i^* = \begin{cases} A_i & \text{if } \mathrm{CTI_i} \geq \max(\mathrm{CTI_x^*}, \mathrm{CTI_{min}}) \\ 0 & \text{if } \mathrm{CTI_i} < \max(\mathrm{CTI_x^*}, \mathrm{CTI_{min}}) \end{cases} \quad \text{(Stocker et al., 2014)}$$

where A_i is the area of pixel *i*, A_x is the total area of each gridcell *x,* and CTI_{min} is the lower threshold for flooding, irrespective of the water table position (Stocker et al., 2014). The maximum potential inundated area fraction in gridcell *x* is then

$$f_x^{\max} = \frac{1}{A_x}\sum_i A_i^* \tag{6}$$

$$\text{with } A_i^* = \begin{cases} A_i & \text{if } \mathrm{CTI_i} \geq \mathrm{CTI_{min}} \\ 0 & \text{if } \mathrm{CTI_i} < \mathrm{CTI_{min}} \end{cases} \quad \text{(Stocker et al., 2014)}$$

The relationship between water table position and flooded area fraction can be approximated by a sigmoidal curve. Stocker et al. (2014) directly define a function, ψ, to approximate this relationship for each distinct gridcell. This reduces computational cost by not relying on the full information contained in the CTI_i values, which constitute a much higher-resolution dataset. For monthly mean values of Γ for each month *m* and gridcell *x*,

$$\psi_x(\Gamma_{x,m}) = \left(1 + v_x e^{-k_x(\Gamma_{x,m} - q_x)}\right)^{-\frac{1}{v_x}} \quad \text{(Stocker et al., 2014).} \tag{7}$$

The flooded area fraction of each gridcell *x* during each month *m* is then calculated as

$$f_{x,m} = \min\left(\psi_x\left(\Gamma_{x,m}\right),\ f_x^{\max}\right) \qquad \text{(Stocker et al., 2014).} \qquad (8)$$

Stocker et al. (2014) note that simple gridcell-average Γ values predicted by many land surface models may be unsuitable for application using this approach, particularly in mineral soils. In CLM, simulated gridcell-average Γ values are generally too low in non-peatland soils (>2m below the soil surface across most of the world) to realistically simulate inundation using this simple scheme. It is therefore necessary to define an "updated" water table position, defined as an index value explicity accounting for the total soil water storage, soil porosity and runoff potential at a given location. We apply such a correction here to derive a new global Γ dataset for use with DYPTOP. This is explained in greater detail in section 2.4.

2.4 Experimental setup

For this work, we examine the link between modelled inundation and CH_4 flux predictions in CLM4Me. To accomplish this, we conduct two separate model simulations: 1) A control case using the model's native GIEMS-derived inundation dataset, and 2) an experimental case in which the inundated fraction is calculated using the DYPTOP spatial parameters and global water table depth predictions generated by CLM. We examine the results over a subtropical subregion of North America, the SE-US, defined as the land surface area between 25° and 37°N latitude and 75° and 55°W longitude. We then compare both sets of results to recent satellite-derived estimates of wetland CH_4 fluxes from Bergamaschi et al. (2013), which are available for the years 2003-2011 and are based on inversions of atmospheric column concentration data.

Both model runs are conducted with the CH_4 sub-model (CLM4Me) active. We use a gridcell resolution of 0.9° x 1.25° and simulated land use conditions for the year

2000. For initial conditions, we use a dataset provided with the model which includes spun-up soil biogeochemistry (CLM4.5-BGC) and atmospheric data derived using the Climate Research Unit analysis of the NCEP atmosphere reanalysis data (CRUNCEP). The model is run off-line using the atmospheric forcing dataset provided with CLM4.5 (Qian et al., 2006). Preliminary trial runs revealed that the model requires ~10-15 years of run-time after the model start date in order for CH_4 emissions to initially stabilize. We therefore initiate both runs beginning in the year 1980 to allow adequate time for the soil carbon stocks to equilibrate ahead of the period for which the inversion estimates are available.

In the control case, inundated surface fraction (f_i) is calculated at each timestep in a manner designed to approximate the GIEMS values. This is done using the inversion approach of Riley et al. (2011), as mentioned above. The experimental case uses an inundation dataset based on global water table depth predicted by CLM (Γ_{CLM}) for one simulation year. We combine these Γ_{CLM} values with predicted values for total soil moisture content, soil porosity and surface runoff to derive a "new" water table depth for use with DYPTOP, following the work of Stocker et al. (2014):

$$\Gamma_m = \frac{1}{N_m}\sum_{d=1}^{N_m}\left(-z_{l_0,d} + \sum_{l=1}^{l_0} W_{l,d} * \frac{\Delta z_l}{\phi}\right) + \frac{\mathrm{runoff_m}}{\phi} \qquad (9)$$

Here, the subscripts m, d, and l represent months, days, and soil layers, with N_m denoting the number of days in month m. $W_{l,d}$ is the daily soil liquid water plus ice fraction in layer l, z_l is the soil layer thickness, ϕ is the porosity (uniform over depth) and runoff_m is the sum of monthly total surface and drainage runoff. l_0 is the number of the layer just above the first frozen soil layer (Stocker et al., 2014).

Since frozen soils tend to occur at mid- to high latitudes, they are not commonly predicted by CLM for the SE-US. We therefore use a simplification of Equation (9)

where the top ten soil layers used in the model (Oleson et al., 2013) are treated as one unfrozen layer, z_{soil}. The value of z_{soil} is the combined thickness of these ten layers and represents the top ~2.865 m of the soil column. We then sum predicted soil moisture for the top ten soil layers using mean monthly values for each layer from an initial 5-year CLM simulation. This allows us to derive a value for monthly soil water content, $W_{l,m}$. Since porosity values vary by soil layer in CLM, we average porosity values at each location over the top ten soil layers to derive ϕ. This gives:

$$\Gamma_{m,\mathrm{new}} = \left(-z_{soil} + \sum_{l=1}^{l_0} W_{l,m} * \frac{\Delta z_l}{\phi}\right) + \frac{\mathrm{runoff_m}}{\phi} \qquad (10)$$

We then apply Equation (7) to calculate ψ_x using these new monthly water table values and the four spatially variable DYPTOP "fit" parameters, which are first interpolated to 0.9° x 1.25° resolution for use with CLM. The monthly inundated fraction of each gridcell is then calculated using Equation (8) and a revised land surface dataset is created using the new inundation values. The CLM4Me model code is then modified so that the new monthly inundated fractions are read at each timestep in place of f_i.

Chapter Three: Results

In general, we find that CH_4 fluxes predicted by CLM4Me over the study region are closely linked to wetland areal extent, in terms of both the magnitude and the spatial distribution of emissions. This is in agreement with findings from the Wetland and Wetland CH_4 Inter-comparison of Models Project (WETCHIMP), which suggest a nearly one-to-one correlation in CLM4Me (Spearman's Rank $\rho = 0.931$) between simulated inundation extent and CH_4 flux prediction globally (Melton et al., 2013). This correlation coefficient was the highest of any of the models in the ensemble. The wetland extent vs. flux correlation in CLM4Me was found to be even higher for the extratropics (latitudes > 35°) with an average ρ-value of 0.980. This value was higher than all of the WETCHIMP models except one, LPJ-WSL (Hodson et al., 2011), which had an extratropical ρ-value of 0.990. One other model, SDGVM (Hopcroft et al. 2011), had a comparable ρ-value for the extratropics (0.979). For CLM4Me, we calculate a ρ-value of 0.841 for northern hemisphere subtropical latitudes (25° - 35°). This strong correlation is observable in a preliminary analysis of the control run results, shown below for the month of June 2003 (Figure 9).

This strong correlation between monthly wetland areal extent and wetland CH_4 flux shows that the calculation of inundation plays an important role in determining the overall flux predicted by CLM4Me. In this section, we analyze the results of the control case, a 35-year CLM model run using the model default land surface dataset that utilizes the GIEMS inundation values. We compare the model results to the satellite inversion estimates of Bergamaschi et al. (2013), which are available for the period 2003-2011.

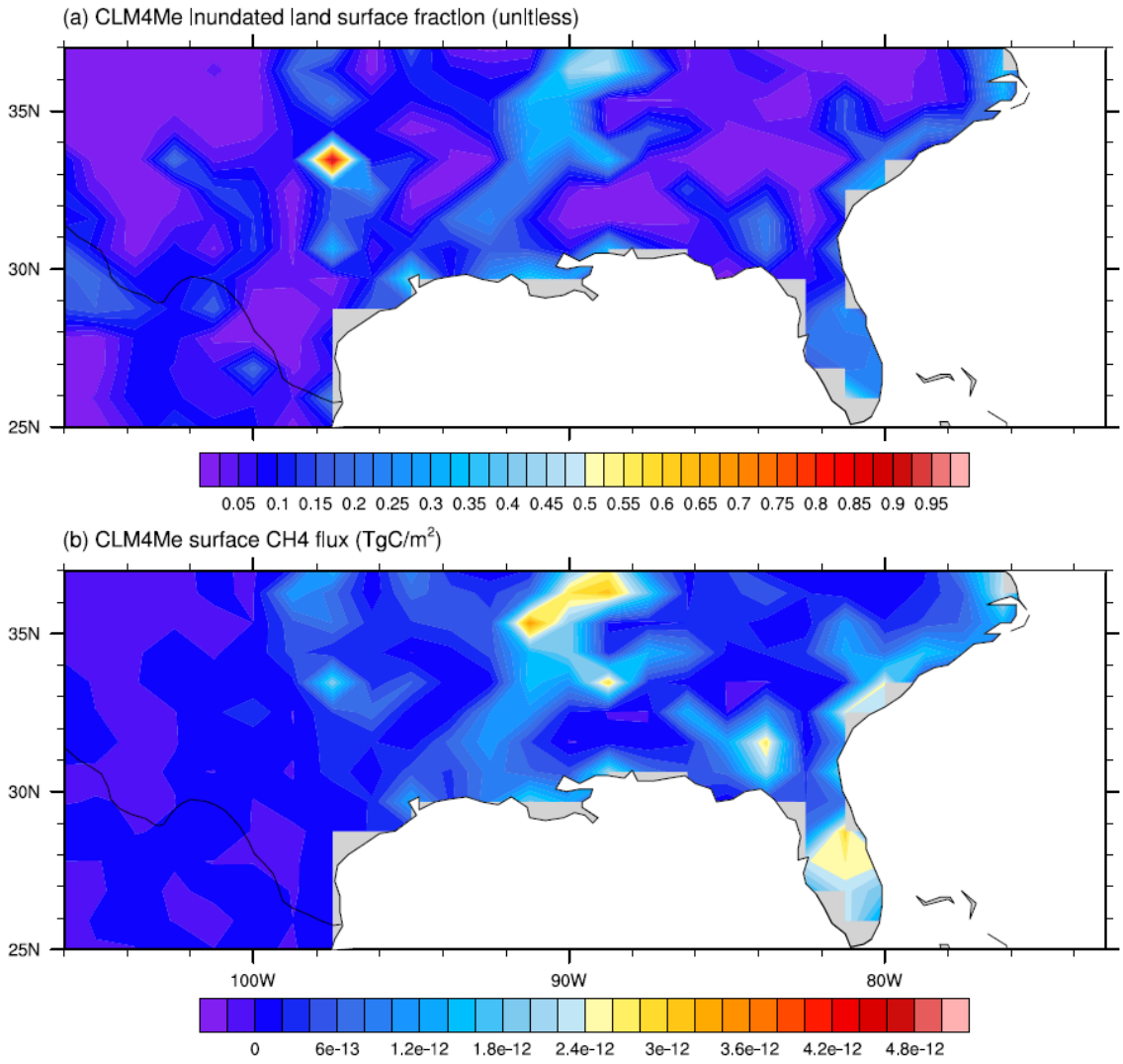

Figure 9: (a) Inundated land surface fraction simulated in CLM4Me for the month of June 2003 and (b) CH_4 flux predicted by CLM4Me for the same month.

3.1 Control case: CLM4Me model results in comparison with satellite inversions

Annual CH_4 flux results in CLM4Me show a strong positive bias over the SE-US in comparison with the SCIAMACHY inversions (Figure 10). In the WETCHIMP model inter-comparison study (Melton et al., 2013) CLM4Me was found to produce CH_4 flux values considerably higher than the ensemble mean for high tropical and subtropical latitudes (25° to 35°) for the study period (1993-2004). A positive bias in flux

predictions over the SE-US is therefore not entirely unexpected. We suggest that much of the bias can be attributed to inundation values used in the model, since (1) the f_i values used by CLM4Me display a slight positive bias over the GIEMS values within the study region, and (2) as noted, the statistical correlation between inundation extent and CH_4 flux in CLM4Me is quite high for subtropical latitudes (Spearman's Rank 0.841).

We note that the inundation values used in CLM4Me are unique; the other models in the WETCHIMP ensemble each use different schemes to simulate inundation. Six of the models, including CLM4Me, utilize the GIEMS values but only one, LPJ-WSL, uses the GIEMS dataset directly to determine wetland areal extent. DLEM (Tian et al., 2010) independently simulates intra-annual wetland dynamics using the GIEMS values for boundary conditions only. ORCHIDEE (Ringeval et al., 2010) uses a TOPMODEL-based scheme but scales simulated wetland areal extent to match the mean annual values of the GIEMS dataset. LPJ-Bern (Spahni et al., 2011) and UW-Vic (Bohn and Lettenmaier, 2010) use prescribed peatland extents in combination with GIEMS monthly inundation values. The other models either simulate inundation extents independently or use prescribed wetland extents from land cover datasets.

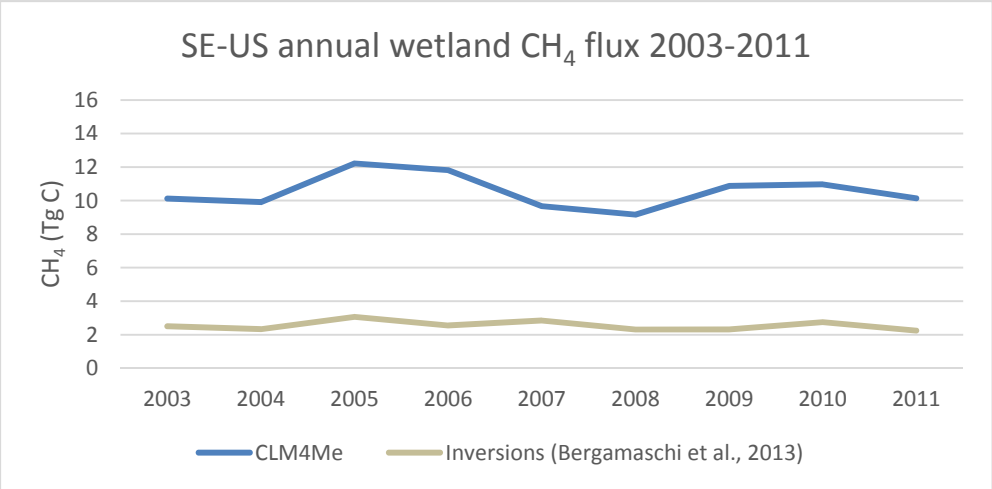

Figure 10: CLM4Me vs. Inversion CH_4 flux values for the period 2003 - 2011 in (fluxes summed over entire study region).

Analyses of the monthly average flux values reveal that much of the positive bias in the yearly totals stems from predictions for July, August and September. CLM4Me predicts fluxes over the SE-US in the range of 1.08 – 1.24 Tg C/month for these months, which are 0.83 – 0.96 Tg C higher than the average values of the inversion estimates for the same three months. In the fall, winter and spring, the bias is still apparent but is reduced; predicted fluxes are in the range of 0.45 – 0.74 Tg C higher than the inversion results (Figure 11).

a)

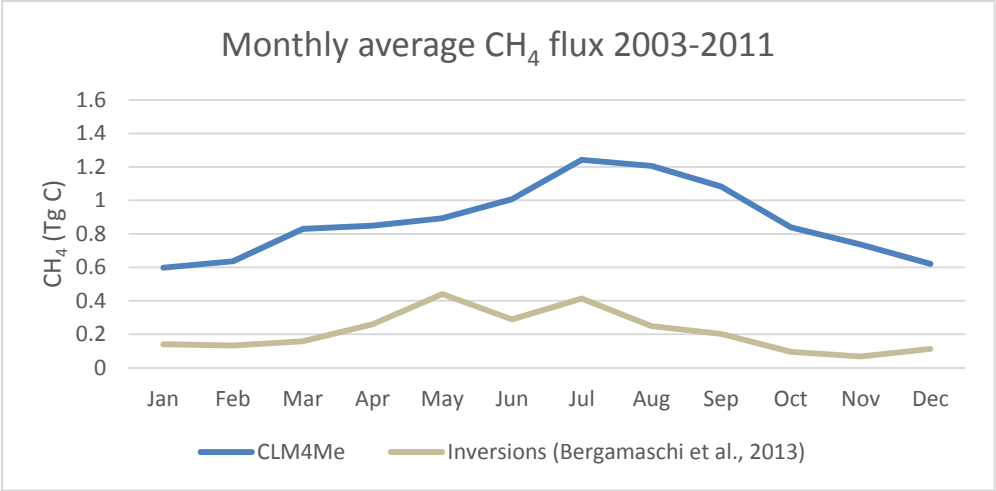

b)

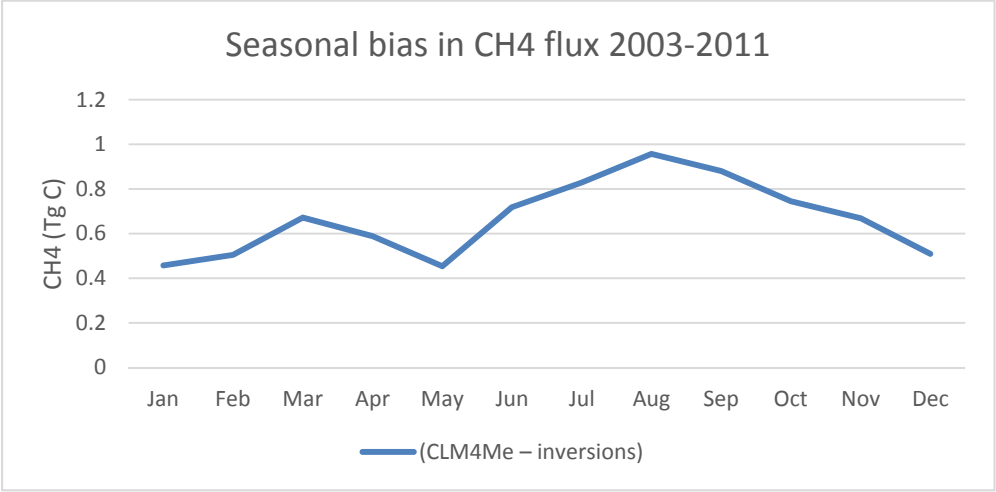

Figure 11: (a) Seasonal variation in CH_4 flux; CLM4Me vs. inversions. (b) Bias (*CLM4Me – inversions*) in predicted monthly values (averaged over 2003 - 2011 for the entire study region).

3.2 Experimental case: CLM4Me with inundation simulated by DYPTOP

Overall, the experimental results reduce the bias for the study region in comparison with the inversion estimates. However, the sign of the bias is reversed from a strong positive bias to a slight negative bias (Figure 12).

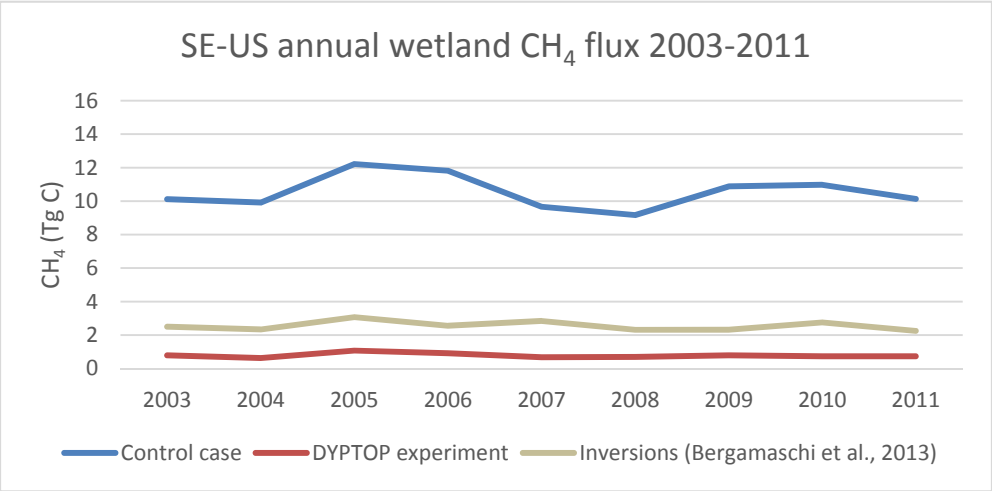

Figure 12: Comparison of SE-US interannual flux predictions; CLM4Me control run, CLM4Me with DYPTOP inundation, and inversion values for the period 2003 - 2011 (fluxes summed over the entire study region).

Since DYPTOP predicts a large (one order of magnitude) decrease in the total inundated fraction throughout the study area (Figure 13), this overall reduction in the magnitude of the predicted emissions is expected, since we establish that flux predictions are closely linked to inundated fraction in CLM4Me.

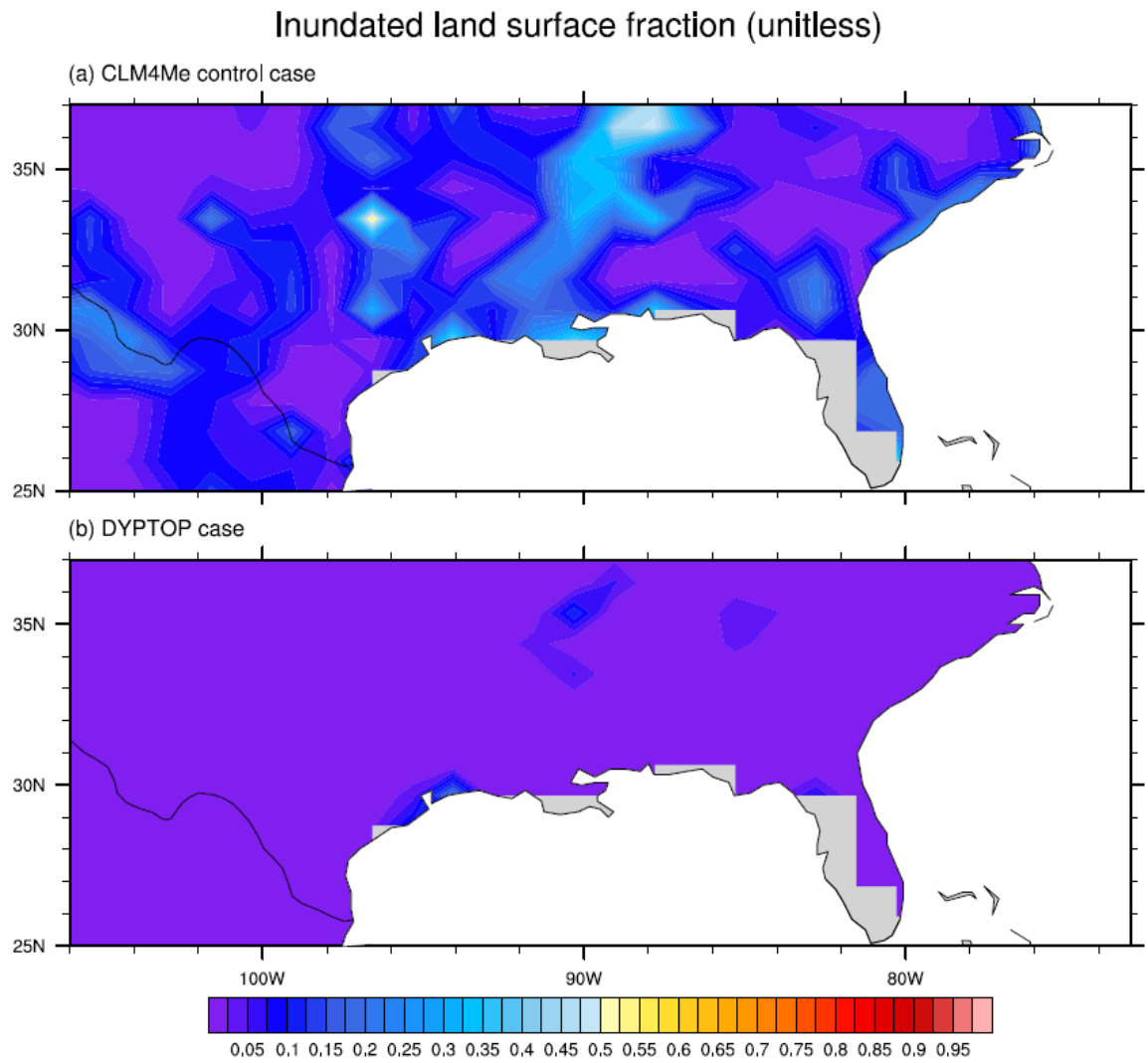

Figure 13: (a) CLM4Me GIEMS-derived fractional inundation values over the study area averaged over all monthly time steps for the period 2003 - 2011. (b) Inundated fraction values using DYPTOP water table and subsequent parameterizations.

In comparison to the control case, much of the negative bias in the annual totals for the experimental case stems from projections for the months of May and July (both ~0.37 Tg C lower than the inversion estimates). However, fluxes are generally well below the inversion values for the period April to September (April, June, August and September predictions are 0.15 – 0.23 Tg C lower than the inversion estimates, while the biases for October through March are only .02 – 0.07 Tg C lower). The inversion results

also imply a sudden, anomalous decrease in SE-US wetland CH_4 emissions during the month of June; May and July emissions are generally the highest of the year, but June emissions are considerably lower. The existence of this June flux anomaly was not suggested by the model.

a)

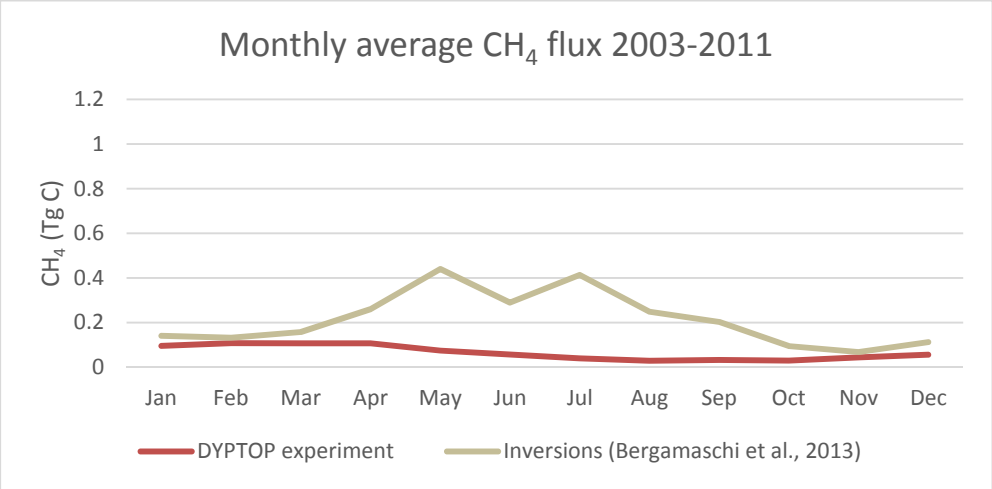

b)

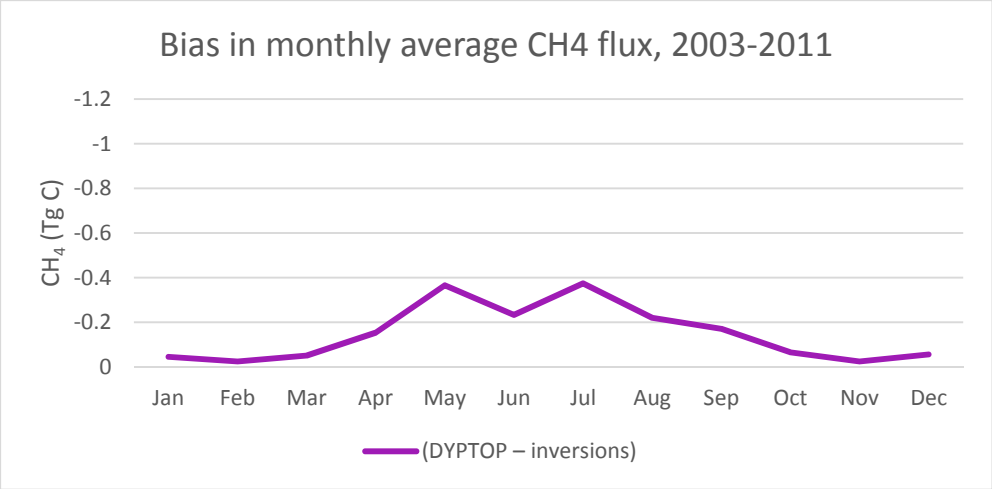

Figure 14: (a) Seasonal variation in CH_4 flux; DYPTOP experiment vs. inversions. (b) Bias (*DYPTOP experiment – inversions*) in predicted monthly values (averaged over the period 2003 - 2011 for the entire study region).

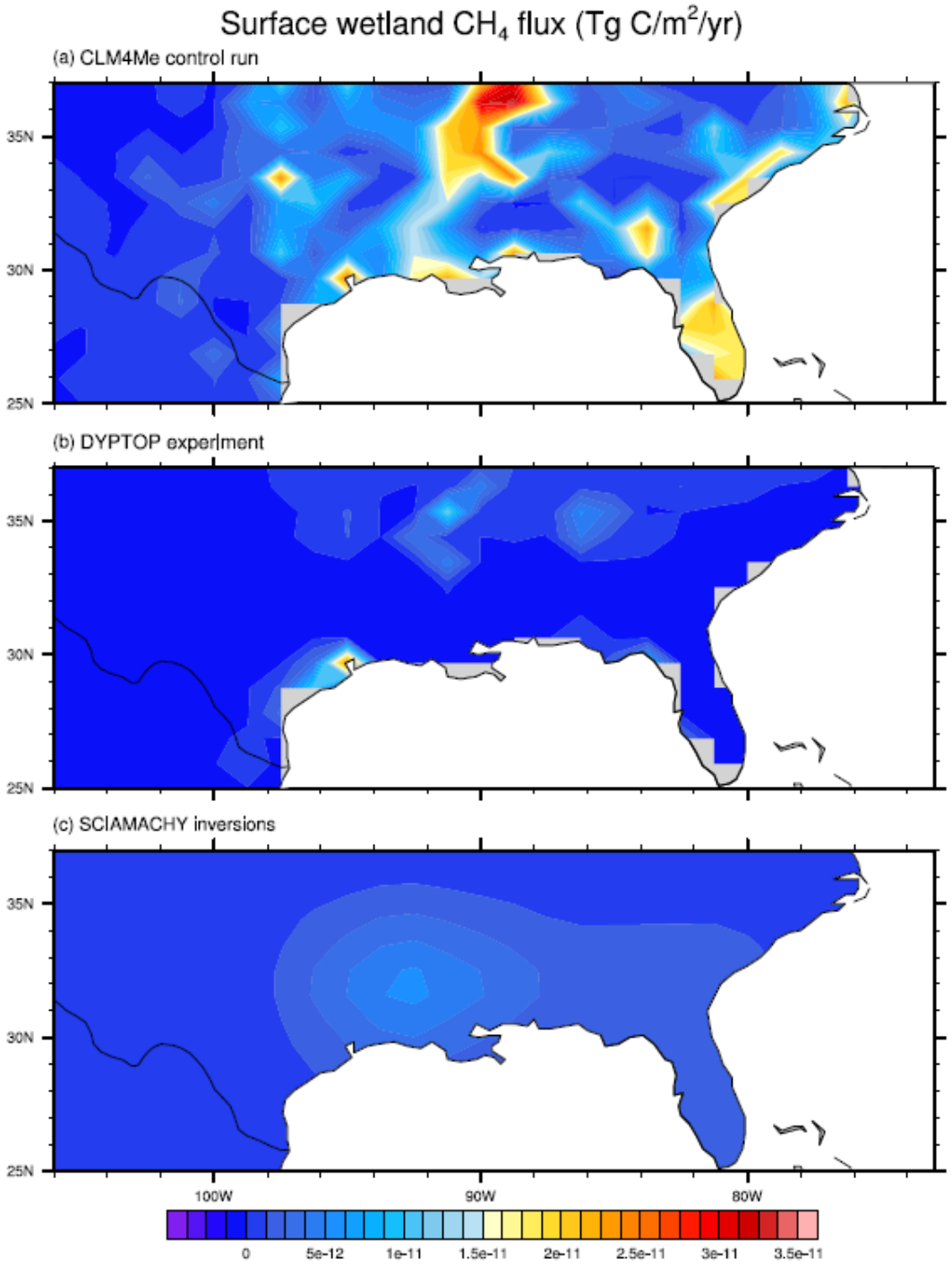

Figure 15: SE-US average wetland CH_4 flux 2003 - 2011 in Tg C/m^2/yr (a) simulated by CLM4Me, (b) simulated using DYPTOP inundation values and (c) based on inversions of ENVISAT-SCIAMACHY satellite retrievals (Bergamaschi et al., 2013).

Spatial analysis of the results reveals that most of the bias reduction in the DYPTOP case comes from lower predicted fluxes over the northern part of the study area that more closely reflect the inversion values. This implies that wet surface conditions may not be as prevalent there as suggested by CLM4Me. However, slight negative bias anomalies observed in the control run over central Georgia, northwestern Louisiana and central Mississippi and Alabama remain unresolved, and a broader negative bias is introduced throughout the lower Mississippi River basin and along the Atlantic Gulf coastal plain (Figure 16). Expected wetter surface conditions in these lower-lying southern areas may therefore not be adequately captured by the DYPTOP implementation. We note, however, missing values in several locations along the Gulf coastline, which preclude a quantitative assessment of the model's performance over this southernmost portion of the study area. This lack of data is an artefact of CLM, which does not explicitly resolve coastal grid cells. Coastal grid cells are instead treated as either land or ocean in the model.

The seasonality of the flux predictions in both cases suggest that accurate representation of summer inundation in the southeastern U.S. plays an important role in determining wetland carbon fluxes on a seasonal and interannual basis. We have made the implicit assumption here that the inversions of Bergamaschi et al. (2013) used for comparison can be taken as a reliable indicator of the magnitude of the true flux. That the inversions show SE-US fluxes to be in the range of 2-3 Tg C per year supports this assumption, since this amount is in good agreement with the other existing regional estimates mentioned in section 1.2.2. Following this assumption, we conclude that the experimental results suggest DYPTOP inundation simulation may greatly improve CH_4 flux predictions in CLM4Me for the fall, winter and spring months.

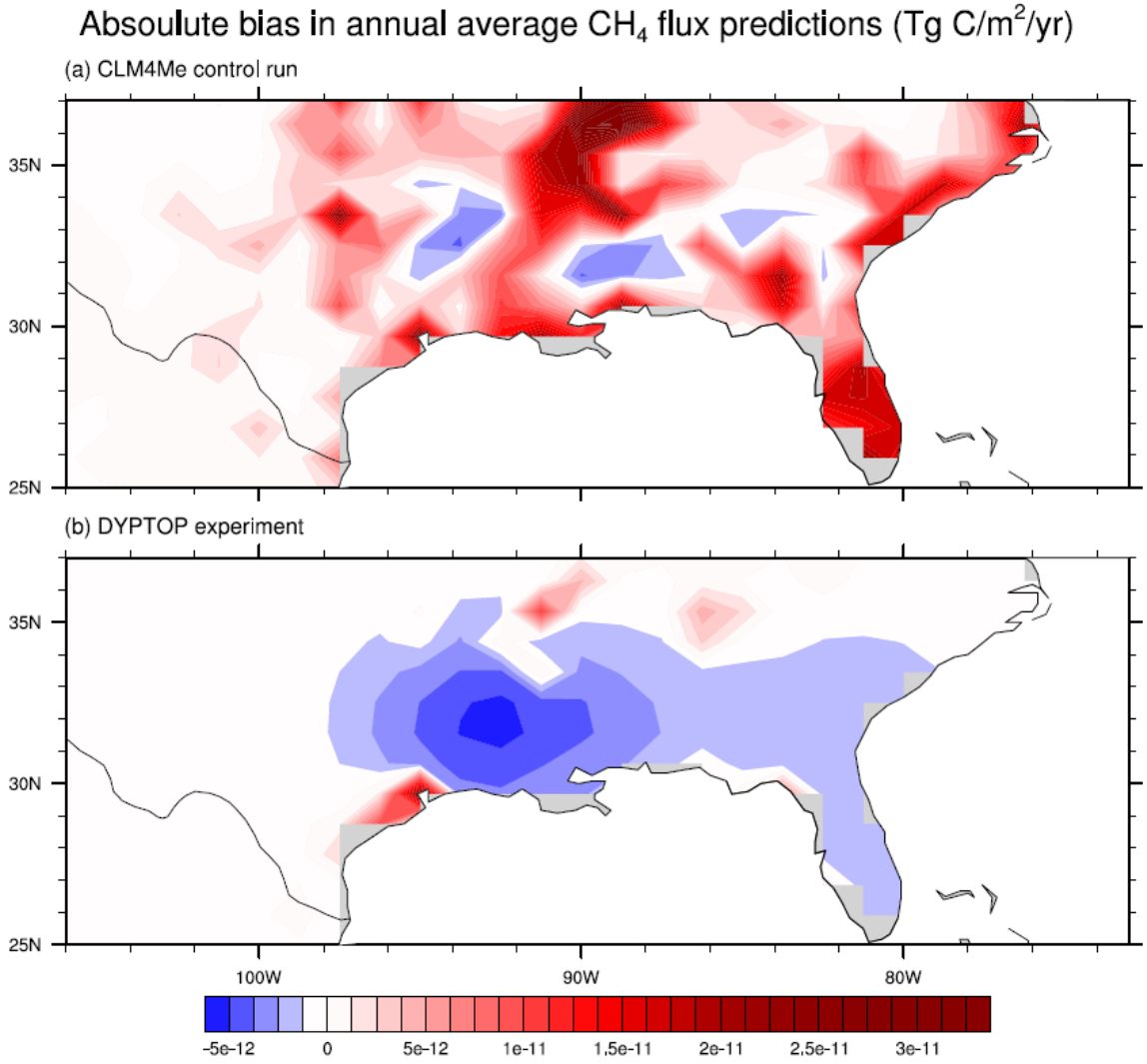

Figure 16: (a) Absolute bias in flux predictions (*experiment – inversions*) averaged over 2003 - 2011 using (a) CLM4Me with default GIEMS-derived fractional inundation vs. (b) CLM4Me with DYPTOP simulated inundation.

In the following section, we attempt a minor modification to the DYPTOP scheme. The aim of the modification is to optimize the inundation dataset for use with CLM4Me such that the model predictions might better mimic the seasonality and the spatial pattern of the inversion estimates.

Chapter Four: Discussion

We have tested the sensitivity of CLM4Me's flux prediction scheme to changes in the amount of surface inundation prescribed to the model. We find wetland areal extent accounts for a high proportion of the seasonal and interannual variability in CH_4 flux simulated by CLM4Me. These findings are in agreement with those of Melton et al. (2013), who show that the correlation between wetland extent and CH_4 emissions in CLM4Me is among the strongest of a suite of wetland-CH_4 models.

Melton et al. (2013) also show that CLM4Me tends to predict the highest annual CH_4 emissions of the ensemble for the latitude range 25° – 27° N, and predicts higher annual emissions than all models except one (DLEM) for the latitude range 27° – 34° N. For latitudes between 27° and 32° N, CH_4 fluxes predicted by CLM4Me are 3 – 5 Tg/yr higher than the ensemble mean. Our finding that CLM4Me predicts annual CH_4 emissions for the SE-US region several Tg higher than existing estimates, including the inversion estimates of Bergamaschi et al. (2013) used as a point of comparison here, is consistent with these results. Anomalously high flux predictions for the study region may be expected since it is defined as between 25° and 37°N latitude (and 75° and 55°W longitude).

Our experimental results imply that for subtropical and low temperate latitudes, the use of a modified inundation scheme can remove some of the bias in modelled fluxes over current satellite-based estimates. However, we also show evidence that inundation and hence flux over the SE-US may be slightly under-predicted using the simplified DYPTOP parameterizations for mineral (non-peatland) soils in combination with CLM's simulated water table (Γ_{CLM}). We therefore propose here a method for further modification, or "optimization," of the inundation scheme such that the model can more realistically prognosticate the flux for any specific region or gridcell. This method may have broader implications for LSM development as future space-based observations produce more reliable data on seasonal inundation and/or surface CH_4 fluxes from

wetlands.

To demonstrate how the DYPTOP scheme may be tuned for use with CLM/CLM4Me, we modify Equation (10) and conduct a separate experiment in which water table depth is calculated based on total soil moisture content, soil porosity, surface runoff, and an additional parameter, *a*, which is used to fit the CLM4Me results to the yearly totals from the inversions for the years 2003-2011:

$$\Gamma_m = \left(-z_{soil} + \sum_{l=1}^{l_0} W_{l,m} * \frac{\Delta z_l}{\phi}\right) + \frac{\mathrm{runoff_m}}{\phi} + a_{m,x} \qquad (11)$$

Here, *a* is an artificial parameter defined as a constant value, in meters, which simply raises (or lowers) the Γ values used to calculate fractional inundation in Equations (7) and (8). This method eliminates the potential for hydrologic balance errors introduced by altering the Γ_{CLM} values in the model itself, since inundation is still calculated independently of Γ_{CLM}. Values of *a* are specific to each gridcell or region for each month, such that a new monthly inundation dataset derived using these values results in fluxes that more closely reflect those of the inversions. Figure (17) shows the results from an example case in which we apply a uniform monthly value of 0.2 for *a* over the entire study region.

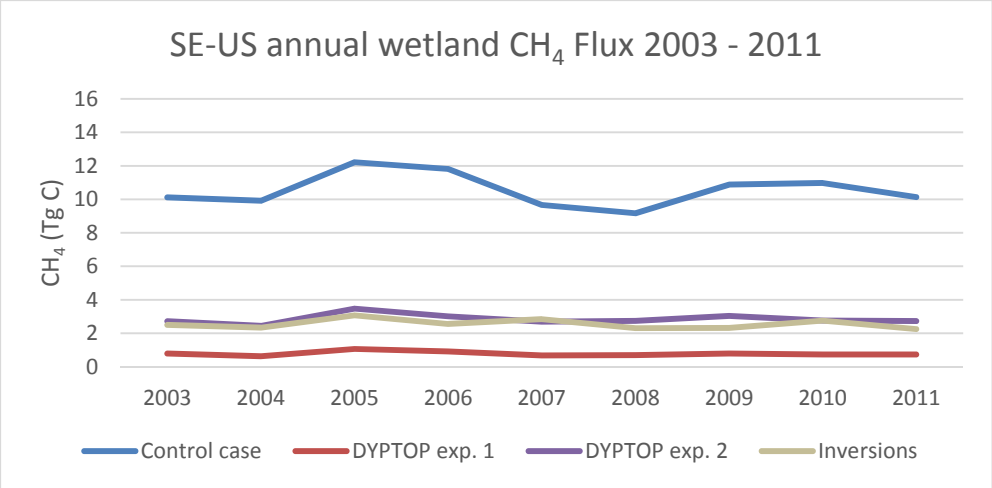

Figure 17: Comparison of SE-US flux predictions (summed over the entire study area); CLM4Me control run, CLM4Me with DYPTOP inundation values, CLM4Me with 20 cm added to adjusted DYPTOP water table values, and inversion values for the period 2003 – 2011.

Although this modification to the DYPTOP scheme greatly reduces the overall bias in the yearly flux totals for the study region as a whole, spatial assessment of the results shows this is due to an increased positive bias over the northern SE-US and a slightly reduced negative bias within the lower Mississippi River basin and along the Gulf coastal plain (Figure 18). The result of this second experiment is encouraging however, since it suggests that a global dataset of *a*-values at sub-regional or gridcell-level scales may be derived using this methodology.

Again, a key assumption made here is that the satellite inversion values realistically represent actual wetland CH_4 fluxes. Since our approach rests on this assumption, Equation (11) does not necessarily optimize the DYPTOP values for more accurate prediction of wetland CH_4 fluxes. Rather, it may be used to tune inundation values such that CLM4Me can better reproduce the inversion results.

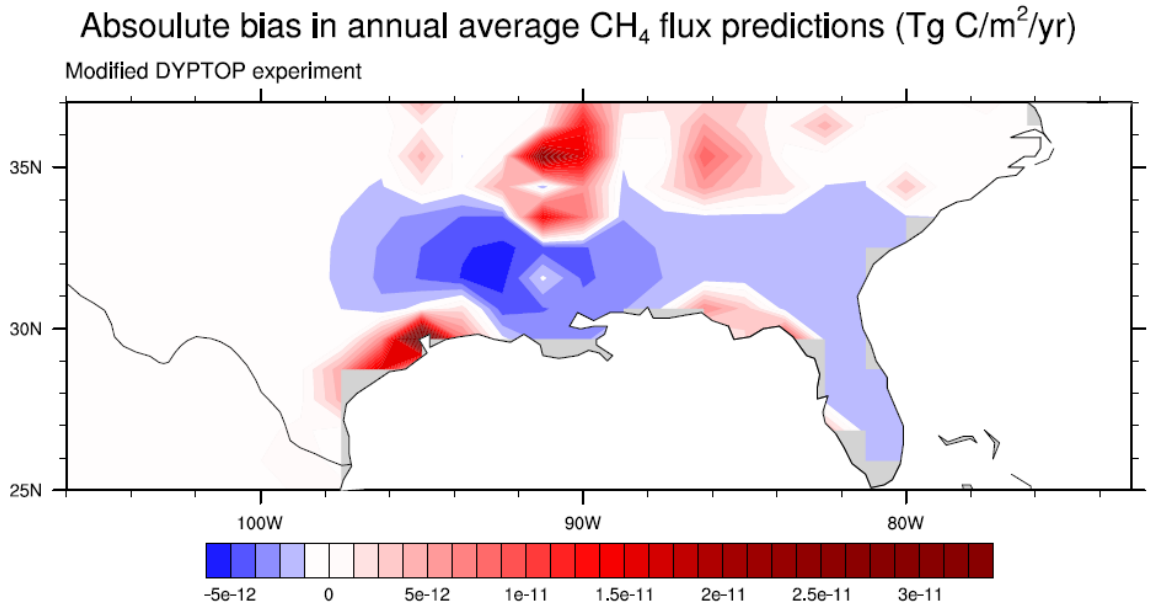

Figure 18: Absolute bias (vs. inversions) in flux predictions averaged over 2003 - 2011 using inundation simulated by DYPTOP with .2m added to adjusted water table values uniformly over the land surface.

Chapter Five: Conclusion

We have conducted a review of recent scientific literature and presented the various environmental factors known to control wetland biogeochemical processes at regional spatial scales. We have emphasized the importance of water table position as a principal controlling factor in wetland CH_4 emissions and discussed the link between surface inundation extent and CH_4 fluxes at seasonal and interannual timescales. We have performed a quantitative first-order assessment of CLM4Me, the CH_4 biogeochemistry component of CLM, over a subtropical wetland region defined as the southeastern U.S. and compared modelled fluxes to recently derived estimates from satellite data in an attempt to clarify the current state of regional-scale wetland CH_4 modeling in LSMs.

We have integrated a new TOPMODEL-based scheme for simulation of wetland areal extent in CLM4Me and examined the link between fractional inundation and modelled surface CH_4 flux. We have shown that, at least for some regions, a simulated inundation scheme based on model-calculated soil hydrologic parameters may be able to more realistically represent surface fluxes than the model's current methodology, which relies on the GIEMS dataset of Prigent et al (2007).

We find that in the CLM4Me model structure, inundation exerts a first-order control on CH_4 flux. Sparse field measurements and coarse space-based observations preclude an assessment of whether this strong dependence on inundation accurately reflects real-world processes. However, we suspect that ongoing research in detecting surface inundation from space – in parallel with improved regional-scale wetland CH_4 flux measurements – will further elucidate the link between inundation and CH_4 emissions for future LSM development. We expect that more quantitative analyses may be possible in the near future as new methods for measuring inundation from space become viable, including, for example, parameterizations based on soil moisture data from NASA's SMAP mission (Brown et al., 2013).

At present, we suggest that the computationally efficient nature of the DYPTOP-derived dynamic inundation scheme presented here has important implications for wetland-CH_4 flux model development; as improved space-based observations become available and can be used to constrain the parameterizations employed by CLM4Me, DYPTOP can be adapted accordingly to more accurately simulate field conditions and to suit CLM4Me's wetland flux scheme. The methodology introduced here therefore represents a relatively straightforward and computationally inexpensive framework for future improvement of inundation simulation in LSMs.

Much work remains to be done toward this end. We note for example one important consideration, mentioned briefly in section 3.2 – the lack of explicit resolution of coastal areas in CLM. Although the study region for this analysis includes coastal southern Florida and Louisiana, areas which represent significant wetland assemblages, CLM does not resolve land surface processes for these areas at 0.9° x 1.25° model resolution. Although higher-resolution model outputs may improve land data coverage somewhat, they are subjected to additional uncertainty and increased computational expense. Regional-scale studies involving global climate models may therefore benefit from supplemental land surface data to populate missing values.

Broadly speaking, however, studies such as this aid in our understanding of the applications and shortfalls of current land surface modeling schemes and represent important strides toward improving model representations of earth system processes. To wit, integration of alternative schemes to simulate inundation and other land surface variables in LSMs may serve to highlight advantages and disadvantages of current model components. Hybrid CH_4 flux models such as the one implemented here can be used to identify potential flaws in a certain model's structure, while employing useful elements of another. We therefore offer this study as a contribution to the current literature and hope that extensions of this work may allow for more sophisticated LSM development in the future.

References

Allen, D. T., V.M. Torres, J. Thomas, D.W. Sullivan, M. Harrison, A. Hendler, S.C. Herndon, C.E. Kolb, M.P. Fraser, A. Daniel Hill, B.K. Lamb, J. Miskimins, R.F. Sawyerand, and J.H. Seinfeld, 2013: Measurements of methane emissions at natural gas production sites in the United States. *Proceedings of the National Academy of Sciences of the United States of America*, *110*(44), 17768–17773. doi:10.1073/pnas.1304880110.

Amante, C., and B.W. Eakins, 2009: ETOPO1 1 Arc-Minute Global Relief Model: Procedures, Data Sources and Analysis. NOAA Technical Memorandum NESDIS NGDC-24. National Geophysical Data Center, NOAA. doi:10.7289/V5C8276M [13 May, 2015].

Bartlett, K.B., and R.C. Harriss, 1993: Review and assessment of methane emissions from wetlands. *Chemosphere*, 26, 1-4, 261-320.

Bergamaschi, P., C. Frankenberg, J.F. Meirink, M. Krol, F. Dentener, T. Wagner, U. Platt, J.O. Kaplan, S. Korner, M. Heimann, E.J. Dlugokencky, and A. Goede, 2007: Satellite chartography of atmospheric methane from SCIAMACHY on board ENVISAT: 2. Evaluation based on inverse model simulations, J. Geophys. Res. Atmos., 112, D02304, doi:10.1029/2006JD007268.

Bergamaschi, P., S. Houweling, A. Segers, M. Krol, C. Frankenberg, R.A. Scheepmaker, E.J. Dlugokencky, S. Wofsy, E. Kort, C. Sweeney, T. Schuck, C. Brenninkmeijer, H. Chen, V. Beck, and C. Gerbig, 2013: Atmospheric CH_4 in the first decade of the 21st century: Inverse modeling analysis using SCIAMACHY satellite retrievals and NOAA surface measurements, *J. Geophys. Res.*, doi:10.1002/jgrd.50480.

Bergman, I., B.H. Svenson, and M. Nilsson, 1998: Regulation of methane production in a Swedish acid mire by pH, temperature, and substrate. Soil Biol. Biochem. 30, 729–741.

Beven, K.J., and M.J. Kirkby, 1979: A physically based, variable contributing area model of basin hydrology, *Hydrolog. Sci. J.*, 24, 43–69.

Bloom, A., P.I. Palmer, A. Fraser, D.S. Reay, and C. Frankenberg, 2010: LargeScale Controls of Methanogenesis Inferred from Methane and Gravity Spaceborne Data, Science, 327, 322–325, doi:10.1126/Science.1175176, 2010.

Bohn, T.J., and D.P. Lettenmaier, 2010: Systematic biases in large-scale estimates of wetland methane emissions arising from water table formulations. Geophys. Res. Lett., 37, 1–6, doi:10.1029/ 2010GL045450.

Boon, P.I., and A. Mitchell, 1995: Methanogenesis in the sediments of an Australian freshwater wetland: comparison with aerobic decay, and factors controlling methanogenesis. FEMS Microbiol. Ecol., 18, pp. 175–190.

Brandt, A.R., G.A. Heath, E.A. Kort, F. O'Sullivan, G. Pétron, S.M. Jordaan, P. Tans, J. Wilcox, A.M. Gopstein, D. Arent, S. Wofsy, N.J. Brown, R. Bradley, G.D. Stucky, D. Eardley, and R. Harriss, 2014: Methane Leaks from North American Natural Gas Systems. *Science,* 343, (6172), 733-735. doi:10.1126/science.1247045.

Bridgham, S.C., and C.J. Richardson, 1992: Mechanisms controlling soil respiration (CO_2 and CH_4) in southern peatlands. *Soil Biol. Biochem*. 24, 1089–1099.

Brown, M.E., V. Escobar, S. Moran, D. Entekhabi, P.E. O'Neill, E.G. Njoku, B. Doorn, and J.K. Entin, 2013: NASA's Soil Moisture Active Passive (SMAP) Mission and Opportunities for Applications Users. *Bull. Amer. Meteor. Soc.*, 94, 1125–1128. doi: http://dx.doi.org/10.1175/BAMS-D-11-00049.1

Bubier, J.L., A. Costello, T.R. Moore, N.T. Roulet, and K. Savage, 1993: Microtopography and methane flux in boreal peatlands, northern Ontario, Canada. *Can. J. Bot.* 71, 1056–1063.

Bubier, J.L., A. Costello, L. Bellisario, N.T. Corner, and P.M. Crill, 1995: Ecological controls on methane emissions from a northern peatland complex in the zone of discontinuous permafrost, Manitoba, Canada. Global Biogeochem. Cycles, 9, 455–470.

Buytaert, W., 2011: Topmodel. Available at: http://cran.r-project.org/web/packages/topmodel/index.html.

Cao, M., J.B. Dent, and O.W. Heal, 1995: Modeling methane emissions from rice paddies. *Global Biogeochem. Cycles*, 9, 183 – 195.

Cao, M., S. Marshall, and K. Gregson, 1996: Global carbon exchange and methane emissions from natural wetlands: Application of a process-based model. J. Geophys. Res. Atmos., 101, 14399 – 14414.

Christensen, T.R., A. Ekberg, L. Stroem, M. Mastepanov, N. Panikov, M. Oequist, B.H. Svensson, H. Nykaenen, P.J. Martikainen, and H. Oskarsson, 2003: Factors controlling large scale variations in methane emissions from wetlands. Geophysical Research Letters 30, (7).

Christensen, T.R. "Wetlands." *Methane and Climate Change.* Ed. Reay, D., Smith P., and van Amstel, A. London: Earthscan, 2010. 27-41.

Crill, P.M., 1991: Seasonal patterns of methane uptake and carbon dioxide release by a temperate woodland soil. *Global Biogeochem. Cycles*, 5, 4, 319-334.

Dahl, T.E., 2005: Florida's Wetlands: An Update on Status and Trends 1985 to 1996. U.S. Department of the Interior, Fish and Wildlife Service, Washington, D.C. 80 pp.

Dahl, T.E., 2011: Status and Trends of Wetlands in the Conterminous United States 2004 to 2009. U.S. Department of the Interior, Fish and Wildlife Service, Washington, D.C. 108 pp.

Dahl, T.E., and S.M. Stedman, 2013: Status and trends of wetlands in the coastal watersheds of the Conterminous United States 2004 to 2009. U.S. Department of the Interior, Fish and Wildlife Service and National Oceanic and Atmospheric Administration, National Marine Fisheries Service. 46 p.

Dunfield, P., R. Knowles, R. Dumont, and T.R. Moore, 1993: Methane production and consumption in temperate and subartic peat soils: Response to temperature and pH. *Soil Biol. Biochem.* 25, 321–326.

Frankenberg, C., J.F. Meirink, M. van Weele, U. Platt, and T. Wagner, 2005: Assessing Methane Emissions from Global SpaceBorne Observations. Science, 308, 5724, 10101014.

Frankenberg, C., P. Bergamaschi, A. Butz, S. Houweling, J.F. Meirink, J. Notholt, A.K. Petersen, H. Schrijver, T. Warneke, and I. Aben, 2008: Tropical methane emissions: A revised view from SCIAMACHY onboard ENVISAT, Geophys. Res. Lett., 35, L15811, doi:10.1029/2008GL034300.

Glenn, S., A. Heyes, and T.R. Moore, 1993: Carbon dioxide and methane fluxes from drained peat soils, southern Quebec. *Global Biogeochem. Cycles* 7, 247–258.

Godfrey, R.K., and J.W. Wooten, 1981: Aquatic and Wetland Plants of Southeastern United States Dicotyledons. Athens, Georgia: The University of Georgia Press.

Goodwin S., and J.G. Zeikus, 1987: Ecophysiological adaptations of anaerobic bacteria to low pH: analysis of anaerobic digestion in acidic bog sediments. *Applied and Environmental Microbiology* 53, 57-64.

Goodwin, S., R. Conrad, and J.G. Zeikus, 1988: Influence of pH on microbial hydrogen metabolism in diverse sedimentary ecosystems. Appl. Environ. Microbiol. 54, 590–593.

Grant, R.F., 1998: Simulation of methanogenesis in the mathematical model Ecosys. *Soil Biol. Biochem.*, 30, 883 – 896.

Grant, R.F., 1999: Simulation of methanotrophy in the mathematical model Ecosys. *Soil Biol. Biochem.*, 31, 287 – 297, 1999.

Grant, R.F., and N.T. Roulet, 2002: Methane efflux from boreal wetlands: Theory and testing of the ecosystem model Ecosys with chamber and tower flux measurements. *Global Biogeochem. Cy.*, 16, 1054, doi:10.1029/2001gb001702.

Hammer-Klose, E.S., and E.R. Thieler, 2001: Coastal Vulnerability to Sea-Level Rise: A Preliminary Database for the U.S. Atlantic, Pacific and Gulf of Mexico Coasts. U.S. Geological Survey Digital Data Series, 68. <http://pubs.usgs.gov/dds/dds68/htmldocs/project.htm>.

Hargreaves, K.J., D. Fowler, C.E.R. Pitcairn, and M. Aurela, 2001: Annual methane emission from Finnish mires estimated from eddy covariance campaign measurements. *Theoretical and Applied Climatology*, 70, 203-213.

Harriss, R.C., D.I. Sebacher, and F.P. JR. Day, 1982: Methane flux in the Great Dismal Swamp. *Nature* **297**, 673–674.

Hodson, E.L., B. Poulter, N.E. Zimmermann, C. Prigent, and J.O. Kaplan, 2011: The El Ni˜no–Southern Oscillation and wetland methane interannual variability, Geophys. Res. Lett., 38, 1–4, doi:10.1029/2011GL046861.

Hopcroft, P.O., P.J. Valdes, and D.J. Beerling, 2011: Simulating idealized Dansgaard-Oeschger events and their potential impacts on the global methane cycle, Quat. Sci. Rev., 30, 3258–3268, doi:10.1016/j.quascirev.2011.08.012.

Kaplan, J.O., 2002: Wetlands at the Last Glacial Maximum: Distribution and methane emissions, Geophys. Res. Lett., 29(6), 1079, doi:10.1029/2001GL013366.

Laine, J., J. Silvola, K. Tolonen, J. Alm, H. Nykänen, H. Vasander, T. Sallantaus, I. Savolainen, J. Sinisalo, and P.J. Martikainen, 1996: Effect of water-level drawdown on global climatic warming: northern peatlands. *Ambio* **25**, 179–184.

Lehner, B., and P. Döll, 2004: Development and validation of a global database of lakes, reservoirs and wetlands. *J. Hydrol.*, 296, 1-22. doi:10.1016/j.jhydrol.2004.03.028.

Martens, C.S., C.A. Kelley, J.P. Chanton, and W.J. Showers, 1992: Carbon and hydrogen isotopic characterization of methane from wetlands and lakes of the Yukon-Kuskokwim Delta, Western Alaska. J. Geophys. Res. 97, 16,689–16,701.

McKenzie, C., S. Schiff, R. Aravena, C. Kelly, and V. St. Louis, 1998: Effect of temperature on production of CH4 and CO2 from peat in a natural and flooded boreal forest wetland. Clim. Change 40, 247–266.

Melton, J.R., R. Wania, E.L. Hodson, B. Poulter, B. Ringeval, R. Spahni, T. Bohn, C.A. Avis, D.J. Beerling, G. Chen, A.V. Eliseev, S.N. Denisov, P.O. Hopcroft, D.P. Lettenmaier, W.J. Riley, J.S. Singarayer, Z.M. Subin, H. Tian, S. Zürcher, V. Brovkin, P.M. van Bodegom, T. Kleinen, Z.C. Yu, and J.O. Kaplan, 2013: Present state of global wetland extent and wetland methane modelling: conclusions from a model inter-comparison project (WETCHIMP). *Biogeosciences*, 10, 753–788.

Miller, S.M., S. Wofsy, A.M. Michalak, E.A. Kort, A.E. Andrews, S.C. Biraud, E.J. Dlugokencky, J. Eluszkiewicz, M.L. Fischer, G. Janssens-Maenhout, B.R. Miller, J.B. Miller, S.A. Montzka, T. Nehrkorn, and C. Sweeney, 2013: Anthropogenic emissions of methane in the United States. *Proceedings of the National Academy of Sciences of the United States of America*, *110*(50), 20018–20022. doi:10.1073/ pnas.1314392110.

Moore, T.R., and N. Roulet, 1995: Methane emissions in Canadian peatlands. *In* R. Lal et al., Eds., Soils and Global Change. Boca Raton, FL: Lewis Publishers, pp. 153–164.
National Oceanic and Atmospheric Administration: *Status and Trends of Coastal Wetlands*. National Marine Fisheries Service, n.d., Web. 10 Mar. 2015.

Niu, G.Y., Z.-L. Yang, R.E. Dickinson, and L.E. Gulden, 2005: A simple TOPMODEL-based runoff parameterization (SIMTOP) for use in global climate models, *J. Geophys. Res.-Atmos.*, 110, D21106, doi:10.1029/2005jd006111.

North American Bird Conservation Initiative, U.S. Committee. 2010: The State of the Birds 2010 Report on Climate Change, United States of America. U.S. Department of the Interior: Washington, DC.

Oleson, K.W., G.Y. Niu, Z.-L. Yang, D.M. Lawrence, P.E. Thornton, P.J. Lawrence, R. Stockli, R.E. Dickinson, G.B. Bonan, S. Levis, A. Dai, and T. Qian, 2008: Improvements to the Community Land Model and their impact on the hydrological cycle, *J. Geophys. Res.-Biogeo.*, 113, G01021, doi:10.1029/2007jg000563.

Oleson, K.W., D.M. Lawrence, G.B. Bonan, B. Drewniak, M. Huang, C.D. Koven, S. Levis, F. Li, W.J. Riley, Z.M. Subin, S.C. Swenson, P.E. Thornton, A. Bozbiyik, R. Fisher, E. Kluzek, J.-F. Lamarque, P.J. Lawrence, L.R. Leung, W. Lipscomb, S. Muszala, D.M. Ricciuto, W. Sacks, Y. Sun, J. Tang, Z.-L. Yang, 2013: Technical Description of version 4.5 of the Community Land Model (CLM). Ncar Technical Note NCAR/TN-503+STR, National Center for Atmospheric Research, Boulder, CO, 422 pp, DOI: 10.5065/D6RR1W7M.

ORNL DAAC: MODIS subsetted land products, 2000. Available at: http://daac.ornl.gov/MODIS/modis.html.

Pacsi, A.P., N.S. Alhajeri, D. Zavala-Araiza, M.D. Webster, and D.T. Allen, 2013: Regional Air Quality Impacts of Increased Natural Gas Production and Use in Texas. *Environ. Sci. Technol.*, 47 (7), 3521–3527. doi:10.1021/es3044714.

Parris, A., P. Bromirski, V. Burkett, D. Cayan, M. Culver, J. Hall, R. Horton, K. Knuuti, R. Moss, J. Obeysekera, A. Sallenger, and J. Weiss, 2012: Global Sea Level Rise Scenarios for the US National Climate Assessment. NOAA Tech. Memo OAR CPO-1. 37 pp.

Pelletier, L., T.R. Moore, N.T. Roulet, M. Garneau, and V. Beaulieu-Audy, 2007: Methane fluxes from three peatlands in the La Grande Riviére watershed, James Bay lowland, Canada. J. Geophys. Res. 112: G01018, doi:10.1029/2006JG000216.

Pickett-Heaps, C. A., D. J. Jacob, K.J. Wecht, E.A. Kort, S. Wofsy, G.S. Diskin, D.E.J. Worthy, J.O. Kaplan, I. Bey, and J. Drevet, 2011: Magnitude of seasonality of wetland methane emissions from the Hudson Bay Lowlands (Canada), Atmos. Chem. Phys., 11(8), 3773–3779, doi:10.5194/acp-11-3773-2011.

Potter, C., J. Bubier, P. Crill, and P. Lafleur, 2001: Ecosystem modeling of methane and carbon dioxide fluxes for boreal forest sites. *Can. J. For. Res.*, 31, 208 – 223.

Potter, C., S. Klooster, S. Hiatt, M. Fladeland, V. Genovese, and P. Gross., 2006: Methane emissions from natural wetlands in the United States: Satellitederived estimation based on ecosystem carbon cycling, Earth Interactions 10: paper 22.

Prigent, C., F. Aires, W.B. Rossow, and E. Matthews, 2001: Joint characterization of vegetation by satellite observations from visible to microwave wavelength: A sensitivity analysis. *J. Geophys. Res.*, 106, 20665–20685.

Prigent, C., F. Papa, F. Aires, W.B. Rossow, and E. Matthews, 2007: Global inundation dynamics inferred from multiple satellite observations, 1993–2000. *J. Geophys. Res.-Atmos.*, 112, D12107, doi:10.1029/ 2006JD007847.

Qian, T., A. Dai, K.E. Trenberth, and K.W. Oleson, 2006: Simulation of global land surface conditions from 1948-2004. Part I. Forcing data and evaluation. *J. Hydrometeorology*, 7, 953-975.

Riley, W.J., Z.M. Subin, D.M. Lawrence, S.C. Swenson, M.S. Torn, L. Meng, N.M. Mahowald, and P. Hess, 2011: Barriers to predicting changes in global terrestrial methane fluxes: analyses using CLM4Me, a methane biogeochemistry model integrated in CESM, Biogeosciences Discuss., 8, 1733–1807, doi:10.5194/bgd-8-1733-2011.

Ringeval, B., N. de Noblet-Ducoudra, P. Ciais, P. Bousquet, C. Prigent, F. Papa, and W.B. Rossow, 2010: An attempt to quantify the impact of changes in wetland extent on methane emissions on the seasonal and interannual time scales. Global Biogeochem. Cy., 24, 1–12, doi:10.1029/2008GB003354.

Roulet, N.T., R. Ash, and W. Quinton, 1993: Methane flux from drained northern peatlands: Effect of a persitent water table lowering on flux. *Global Biogeochem. Cycles* **7**, 749–769.

Schimel, J.P., 1994: Plant transport and methane production as controls on methane flux from arctic wet meadow tundra. *Biogeochemistry* 28, 183-200, 1995.

Sebacher, D.I., R.C. Harriss, and K.B. Bartlett, 1985: Methane emissions to the atmosphere through aquatic plants. *J. Env. Qual.* 14(1), 40-46.

Segers, R. 1998: Methane production and methane consumption: A review of processes underlying wetland methane fluxes. *Biogeochemistry* 41, 23–51.

Shaw, Ethan: *Names of Wetlands in the Southeast*. <http://traveltips.usatoday.com/names-wetlands-southeast-108670.html>.

Spahni, R., R. Wania, L. Neef, M. van Weele, I. Pison, P. Bousquet, C. Frankenberg, P.N. Foster, F. Joos, I.C. Prentice, and P. van Velthoven, 2011: Constraining global methane emissions and uptake by ecosystems. Biogeosciences, 8, 1643–1665, doi:10.5194/bg-8-1643-2011.
Stocker, B.D., R. Spahni, and F. Joos, 2014: DYPTOP: a cost-efficient TOPMODEL implementation to simulate sub-grid spatio-temporal dynamics of global wetlands and peatlands. *Geosci. Model Dev*., 7, 3089–3110.

Svensson, B.H., 1984: Different temperature optima for methane formation when enrichments from acid peat are supplemented with acetate or hydrogen. *Appl. Environ. Microbiol.* 48, 389–394.

Svensson, B.H., and T. Roswall, 1984: In situ methane production from acid peat in plant communities with different moisture regimes in a subarctic mire. Oikos 43, 341–350.
Tian, H., X. Xu, M. Liu, W. Ren, C. Zhang, G. Chen, and C. Lu, 2010: Spatial and temporal patterns of CH4 and N2O fluxes in terrestrial ecosystems of North America during 1979–2008: application of a global biogeochemistry model. Biogeosciences, 7, 2673–2694, doi:10.5194/bg-7-2673-2010, 2010.

Tokida, T., T. Miyazaki, M. Mizoguchi, O. Nagata, F. Takakai, A. Kagemoto, and R. Hatano, 2007: Falling atmospheric pressure as a trigger for methane ebullition from peatland. *Glob. Biogeochem. Cy.* 21: GB2003, doi:10.1029/2006GB002790.

Treat, C.C., J.L. Bubier, R.K. Varner, and P.M. Crill, 2007: Time scale dependence of environmental and plant- mediated controls on CH4 flux in a temperate fen. J. Geophys. Res. 112: G01014, doi:10.1029/2006JG000210.

U.S. Department of Agriculture, 2013: *Summary Report: 2010 National Resources Inventory*. Natural Resources Conservation Service, Washington, DC, and Center for Survey Statistics and Methodology, Iowa State University, Ames, Iowa.

U.S. Environmental Protection Agency, 2010: *Methane and nitrous oxide emissions from natural sources*. Office of Atmospheric Programs, Eastern ResearchGroup, Inc. Washington, D.C.

U.S. Fish and Wildlife Service, 2014: National Wetlands Inventory website. U.S. Department of the Interior, Fish and Wildlife Service, Washington, D.C. http://www.fws.gov/wetlands/.
Valentine, D.W., E.A. Holland, and D.S. Schimel, 1994: Ecosystem and physiological controls over methane production in northern wetlands, J. Geophys. Res., 99, 1563–1571.

Walter, B.P., M. Heimann, and E. Matthews, 2001: Modeling modern methane emissions from natural wetlands. Model description and results, *J. Geophys. Res.-Atmos.*, 106, 34189–34206.

Wecht, K.J., D.J. Jacob, C. Frankenberg, Z. Jiang, and D.R. Blake, 2014: Mapping of North American methane emissions with high spatial resolution by inversion of SCIAMACHY satellite data, J. Geophys. Res. Atmos., 119, 7741–7756, doi:10.1002/2014JD021551.

Westerman, P., 1993: Temperature regulation of methanogenesis in wetlands. Chemosphere 26, 321–328.

Whalen, S.C., 2005: Biogeochemistry of methane exchange between natural wetlands and the atmosphere. Environ. Eng. Sci. 22(1): 73-94.

Whiting, G.J., and J.P. Chanton, 1992: Plant-dependent CH4 emission in a subarctic Canadian fen. *Global Biogeochem. Cycles* 6(3): 225-231.

Whiting, G.J., and J.P. Chanton, 1993: Primary production control of methane emission from wetlands. *Nature* 364, 794-795.

Williams, R.T., and R.L. Crawford, 1985: Methanogenic bacteria, including an acid-tolerant strain, from petalands, Appl. Environ. Microbiol., 50, 1542–1544.

Wofsy, S., and R.C. Harriss, 2002: The North American Carbon Program (NACP). Report of the NACP Committee of the U.S. Interagency Carbon Cycle Science Program, U.S. Global Change Research Program, Washington, DC, 75 pp.

Wong, P.P., I.J. Losada, J.-P. Gattuso, J. Hinkel, A. Khattabi, K.L. McInnes, Y. Saito, and A. Sallenger, 2014: Coastal systems and low-lying areas. In: *Climate Change 2014: Impacts,Adaptation, and Vulnerability. Part A: Global and Sectoral Aspects. Contribution of Working Group II to the Fifth Assessment Report of the Intergovernmental Panel on Climate Change* [Field, C.B., V.R. Barros, D.J. Dokken, K.J. Mach, M.D. Mastrandrea, T.E. Bilir, M. Chatterjee, K.L. Ebi, Y.O. Estrada, R.C. Genova, B. Girma, E.S. Kissel, A.N. Levy, S. MacCracken, P.R. Mastrandrea, and L.L.White (eds.)]. Cambridge University Press, Cambridge, United Kingdom and New York, NY, USA, pp. 361-409.

Yavitt, J.B., C.J. Williams, and R.K. Wieder, 1997: Production of methane and carbon dioxide in peatland ecosystems across North America: Effects of temperature, aeration, and organic chemistry of peat. *Geomicrobiol. J.* 14, 299–316.

Yavitt, J.B., C.J. Williams, and R.K. Wieder, 2000: Controls on microbial production of methane and carbon dioxide in three Sphagnum-dominated peatland ecosystems as revealed by a reciprocal field peat transplant experiment. *Geomicrobiol. J.* 17, 61–88.

Zeikus, J.G., and M.R. Winfrey, 1976: Temperature limitation of methanogenesis in aquatic sediments. *Appl. Environ. Microbiol.* 33, 275–281.

Zhang, Y., C. Li, C.C. Tretin, H. Li, and G. Sun, 2002: An integrated model of soil, hydrology, and vegetation for carbon dynamics in wetland ecosystems. *Global Biogeochemical Cycles*, Vol. 16, NO. 4, 9-1—9-17.

Zhuang, Q., J.M. Melillo, D.W. Kicklighter, R.G. Prinn, A.D. McGuire, P.A. Steudler, B.S. Felzer, and S. Hu, 2004: Methane fluxes between terrestrial ecosystems and the atmosphere at northern high latitudes during the past century: A retrospective analysis with a process based biogeochemistry model. *Global Biogeochem. Cycles,* 18**,** GB3010, doi:10.1029/2004GB002239.